FINAL TECHNICAL REPORT

LIDAR AND FIELD MAPPING OF QUATERNARY FAULTS IN THE U.S. TERRITORY OF GUAM

Prepared for
U.S. Geological Survey
National Earthquake Hazards Reduction Program
Award Number G11AP20058

July 2015

URS Corporation
Seismic Hazards Group
1333 Broadway, Suite 800
Oakland, California 94612

FINAL TECHNICAL REPORT

LIDAR AND FIELD MAPPING OF QUATERNARY FAULTS IN THE U.S. TERRITORY OF GUAM

Principal Investigators
Judith Zachariasen
Susan Olig
URS Corporation
(Award G09AP00048)
1333 Broadway, Suite 800, Oakland, CA 94612
(510) 874-1749 (phone); (510) 874-3268 (fax);
judy_zachariasen@urs.com

Program Elements I and III
Northern California Region

Keywords:
Quaternary fault behavior, neotectonics, paleoseismology

U. S. Geological Survey
National Earthquake Hazards Reduction Program
Award Number G11AP20058

July 2015

This research was supported by the U.S. Geological Survey (USGS), Department of the Interior, under USGS Awards G11AP20058. The views and conclusions contained in this document are those of the Principal Investigators only and should not be interpreted as necessarily representing the official policies, either expressed or implied, of the U.S. Government.

ABSTRACT

The U.S. territory of Guam is the largest, most-populated, and southernmost of the Mariana Islands, a chain of volcanic islands and seamounts that constitute the Mariana Arc, and it lies in the midst of a complex plate boundary zone in the western Pacific Ocean. Guam is located on the Mariana plate, a microplate of the Philippine Sea plate, and is flanked on the east and southeast by the Mariana subduction zone, on the west by an active spreading center, and on the south by a series of right-lateral transform faults. Several large historic earthquakes, including an **M** 7.7 event in the Mariana subduction zone in 1993, have affected Guam. Furthermore, there are numerous surface faults on the island that appear to displace Quaternary materials. The tectonic setting and the presence of Quaternary faults suggest that Guam could face a significant seismic hazard from the subduction zone and/or crustal faults. Little work to date, however, has been done in identifying and assessing the seismic potential of the crustal faults. This proposal aims to address the lack of data about onshore Quaternary faults in Guam with the goal of providing more accurate information about the sources that contribute to Guam's seismic hazard.

The reports presents a new map of the Quaternary faults of Guam. Based on analysis of island-wide Lidar, bathymetric data, aerial photographs, and field mapping we have compiled, at a scale of 1:50,000, a map of lineaments that do or may represent Quaternary faults. We also include a compilation of fault data where obtainable, including geometry, sense of slip, and level of activity. This map of Guam's active faults may be used as a first step in characterizing the onshore sources of seismic hazard.

TABLE OF CONTENTS

LIST OF TABLES AND FIGURES

1.0 INTRODUCTION

Guam, a U.S. territory, is the largest and southernmost of the Mariana Islands, a chain of volcanic islands and seamounts that constitute the Mariana Arc (Figure 1). It is located on the Mariana plate, a microplate of the Philippine Sea plate, between an active subduction zone and a spreading center. As such, it is in a tectonically active region that is the locus of seismic activity. Several large historic earthquakes have affected Guam, and there are numerous surface faults on the island that appear to displace Quaternary materials. The tectonic setting and the presence of Quaternary faults suggest that Guam could face a significant seismic hazard from the subduction zone and/or the onshore faults. Any thorough seismic hazard assessment should include characterizations of both regional and local sources. To date, no modern field-based map of the active faults of Guam exists, and there is very little information about the age of fault activity.

In this project, we have begun to address the paucity of data about onshore crustal fault characteristics by undertaking a detailed Lidar and field mapping investigation of the Quaternary faults on Guam to identify them, accurately determine their location, characterize their sense of slip, and obtain preliminary information regarding their level of activity. We have developed map of Guam’s active faults at a scale of 1:50,000 as a first step in better characterizing the crustal sources of seismic hazard. We have also developed preliminary characterizations of some of Guam's fault for use in seismic hazard assessment.

2.0 TECTONIC SETTING

The Mariana volcanic arc results from the northwestward subduction of the Pacific plate beneath the Philippine Sea plate at the Mariana Trench, located south and east of Guam (EERI, 1995) (Figure 1). This subduction zone is the source of many of the earthquakes affecting Guam (EERI 1995; Somerville, 2000). The Mariana Trench is notably arcuate and at its southern end changes strike from near north-south at about latitude 16°N to about N77E at latitude 11°N, south of Guam. In the same region, the Benioff-Wadati zone varies considerably along strike, changing from a near vertical zone extending to 600 km depth north of 15°N latitude to a moderately dipping zone extending only to about 200 km at the south end of the trench (Dames and Moore, 1994). The Mariana subduction zone has been identified as unlikely to produce great earthquakes as a consequence of its steep dip and low degree of coupling (Ruff and Kanamori, 1980; Pacheco *et al*., 1993), but at its southern end, where the dip shallows, it may be more strongly coupled and capable of producing larger earthquakes. Indeed, the occurrence of an **M** 7.7 earthquake on the subduction interface in 1993 (Somerville, 2000) indicates that it is seismogenic.

West of Guam, a north-south trending spreading center in the Mariana Trough back-arc basin forms the western edge of the Mariana microplate (Figure 1). This spreading center is opening east-west at a half rate of less than 2 cm/year (Hussong and Uyeda, 1981). This half spreading rate, combined with approximately 3 mm/yr of Pacific-Philippine Sea plate convergence, yields a total relative convergence rate between the Mariana plate and the Pacific plate of about 5 cm/yr north of about 12.5°N latitude. South of this latitude, the Mariana Trough spreading stops and the convergence rate between the Mariana and Pacific plates decreases to about 3.5 cm/yr. Seismicity in the trough region is relatively low compared to the subduction zone, but earthquakes larger than body-wave magnitude (m_b) 5.0 have occurred historically (Eguchi, 1984).

South of Guam a series of large east-northeast-trending fracture zones and right-lateral transform faults truncate the southern end of the Mariana Trough and link it to the Mariana Trench (Karig *et al*., 1978; Rankin *et al.*, 1984). These faults likely help accommodate the dextral component of the oblique convergence that occurs at the southern end of the Mariana subduction zone where it curves into a more easterly strike (Dames and Moore, 1994).

2.1 Regional Seismicity

Guam has repeatedly experienced strong ground shaking from earthquakes. Given its location on the overriding plate of a subduction zone, these have probably included earthquakes on the subduction interface, within the downgoing Pacific plate, and within the overriding Mariana plate. Earthquakes within the overriding plate could be generated by rupture of crustal faults on Guam. However, no historic or prehistoric earthquake has yet been identified with any such fault.

The most significant recent earthquake on Guam occurred on August 8, 1993. This M_S 8.1 (**M** 7.7) event occurred 50 km south of Guam at a depth of 60 km along the Mariana Trench. Initially there was debate as to the source of this earthquake (EERI, 1995), but evidence from a recent study of aftershocks (Somerville, 2000) suggests that it occurred on the interface between the Pacific plate and the Mariana plate. Buildings were damaged or destroyed throughout the island. The preliminary estimate of damage to commercial buildings was $112 million.

One federally-declared earthquake disaster has occurred on Guam. On October 12, 2001, a **M** 7.3, maximum Modified Mercalli (MM) intensity VII earthquake struck Guam. This earthquake was believed to have caused one injury, but no published estimates of total damage are available. Many buildings were damaged, including several schools in Santa Rita and Piti, and utilities were disrupted (USGS, 2004). Information on other significant Guam earthquakes is described in URS (2005).

Focal mechanisms of earthquakes near Guam indicate a complex mix of faulting as might be expected at the juncture of multiple active plate boundaries. Reverse faulting dominates the boundary between the Pacific and Mariana Plates, resulting from compression perpendicular to the plate boundary (northwest near Guam). This northwest compression is consistent with convergence of the Pacific and Mariana plates along the Mariana subduction zone. A few normal faulting earthquakes also occur along the plate boundary, which may be caused by extension in the hinge of the subducting plate. Normal faulting earthquakes also occur west of Guam as a result of extension along the spreading ridge between the Mariana and Philippine Sea plates. Finally, a few strike-slip faulting earthquakes have occurred in various locations throughout the region. Some of these may be occurring on strike-slip faults within plates and some are accommodating lateral movement on complex zones and irregularities along plate boundaries.

2.2 Geology of Guam

Guam, along with the islands of Rota, Saipan, and Farallon de Medinilla to the north, is part of the Mariana island arc that is now volcanically inactive (Figure 1). Volcanic activity on Guam began about 43 million years ago and ceased about 15 million years ago (Tracey *et al.*, 1964; Siegrist *et al.*, 1998). Since that time, extensive development of coral reefs and lagoons has resulted in periodic deposition of coralline reef and detrital limestone, particularly in northern Guam and along the island perimeter (Tracey *et al.*, 1964). As a result of continued uplift of the island, probably related to convergence and earthquakes along the Mariana subduction zone, extensive paleo-reefs and lagoons have completely emerged and are sub-aerially exposed in the island interior. Modern reef development continues in the coastal areas along the island perimeter. This geologic history has resulted in the two major physiographic provinces evident on Guam today, a broad generally flat, uplifted plateau region that is dominantly Plio(?)-Pleistocene limestone in the north and a highly dissected more mountainous Eocene to Pliocene volcanic terrain to the south (Figure 2). These are separated by the west-northwest-striking Adelup fault, which bisects the island.

2.3 Crustal Faults

Numerous faults transect the island of Guam, but their mapping, at least as late Quaternary structures, has been rudimentary. Tracey *et al.* (1964) first mapped them as part of an island-wide bedrock geologic map study that was actually conducted pre-plate tectonics. Dames & Moore (1994) remapped the faults, with an emphasis on evaluating their earthquake potential, using the Tracey *et al*. map and aerial photograph interpretation but little or no field investigation. The most prominent faults include the Adelup, Talofofo, Mount Santa Rosa (including the Machanao fault as shown on Figure 2), Tamuning-Yigo, Cabras, and Cocos faults as well as a suite of faults near Aga Point at the southeast tip of Guam. With the exception of the Cabras and Tamuning-Yigo faults, all the faults strike northwest. The Tamuning-Yigo fault strikes east-northeast, and the Cabras fault strikes north-northeast. Both the Cabras and Tamuning-Yigo faults appear to be truncated by northwest-striking faults, and therefore may be older.

Tracey *et al.* (1964) mapped all the above faults as normal faults. Dames and Moore (1994) determined that they all show evidence for normal slip, but many may also have a significant strike-slip component. In fact, the sense of slip on these faults is poorly known, largely because they have not been extensively examined with an eye to their Quaternary characteristics and activity. One of the few faults that has been examined in detail in the field, the Tamuning-Yigo fault, has characteristics of both normal faulting and reverse-oblique faulting along various sections (Olig *et al.*, 2007). Given the tectonic setting, faults of any slip sense might be expected in Guam. Characterizing the sense of slip on the Quaternary faults is crucial for developing a meaningful seismic hazard characterization or a seismic hazard map.

2.4 Quaternary Geology and Tectonics

Although Tracey *et al.* (1964) mapped the bedrock geology of Guam at a 1:50,000 scale (their Plate 1) and Dames & Moore (1994) mapped Quaternary sediments at the same scale in an effort to assess seismic hazard (their Plate 1), little is known about the absolute ages of Quaternary deposits on Guam. The northern plateau comprises primarily Plio(?)-Pleistocene Mariana limestone. A series of marine terraces have been cut into and are clearly younger than the Mariana limestone. Some of the lowest terraces have a veneer of Merizo limestone whose age is between about 2750 and 4250 BP, based on 14C dating of corals (Randall and Siegrist, 1996). This limestone likely formed during the mid-Holocene sea-level high stand and currently is exposed at elevations of 1-4 m. The mid-Holocene highstand in the Marianas occurred about 5,000 BP, followed by a drawdown in sea level until about 3,000 BP, when it stabilized near modern sea level (Dickinson, 2000; Kayanne et al., 1993; Randall and Siegrist, 1996). The Late Pleistocene Tarague limestone, a fossil reef, has only a limited occurrence, restricted to the north coast in Tarague embayment (Miklavic, 2011; Siegrist et al., 2007). It has been dated to 126-139 ka, and thus formed during marine isotope stage 5e interglacial highstand (Randall and Siegrist, 1996; Miklavic, 2011). It is found at elevations of 3-8 m, but its surface has been denuded (Miklavic, 2011).

Using the Tracey *et al.* (1964) map and aerial photographs, Dames & Moore (1994) identified six to eight uplifted marine terraces, as high as 82 m above sea level, along the perimeter of Guam, and produced a series of topographic profiles across the terrace flights at several locations around the island. From approximate correlations to global paleo-sea level curves, they estimated terrace ages to range from a few thousand to over 120,000 years, yielding uplift rates as high as 1.55 mm/yr in northern Guam. Randall and Siegrist (1996) identified 3 to 6 uplifted terraces, and for those between 10 and 200 m elevation, they estimated ages between 125,000 and 2 million years old, yielding uplift rates an order of magnitude lower. The presence of last interglacial Tarague Limestone at elevations of 3-8 m in Tarague Embayment on the north coast suggests the lower rates are more accurate.

The constraints on the age of deformation and faulting in Guam are minimal. The terraces cut into the Mariana limestone are exposed above modern sea level at differing elevations around the island indicating that the island has been uplifted and tilted in the late Quaternary. The Holocene(?) Merizo limestone veneer appears at elevations of about 1 m in the south and 4 m in the north, suggesting some deformation has occurred in the Holocene (Dames and Moore, 1994; Randall and Siegrist, 1996; Miklavic, 2011). Dames and Moore (1994) report evidence for late Quaternary (≤ 130,000 years) activity on several crustal fault zones including the Adelup, Talofofo, Mount Santa Rosa, Tamuning-Yigo, Cabras, and Cocos faults. They also cite Siegrist (written communication) for evidence of late Quaternary activity on faults near Aga Point. These faults appear to deform the late Quaternary marine terraces that ring the island and in some cases appear to offset likely Holocene deposits.

Dames and Moore (1994) used elevation profiles of the terraces and global sea-level curves to infer uplift rates at numerous locations around the island. They found overall uplift rates for the island of 0.4-0.9 mm/yr. They interpreted variations in uplift rate and degree of tilting at different locations across the faults as evidence of late Quaternary slip on those faults, but did not examine the mapped faults directly for evidence of slip. Inferred slip rates across the main crustal faults ranged from 0.2 to 0.5 mm/yr, slip rates that are consistent with faults that generate moderate earthquakes with recurrence intervals on the order of a few thousand years.

As is often the case in areas where the historical seismicity record is short, no surface-rupturing earthquakes are known to have occurred historically on any of the faults mapped on Guam, despite the geologic evidence of prehistoric late Quaternary surface faulting.

2.5 Fault Characterization

Additional study is greatly needed to better understand fault geometries, kinematics, rates of activity and paleoseismicity in Guam. Further investigation of the marine terraces and ages of Quaternary deposits is also needed to better constrain ages of fault activity and better understand the relation of island uplift to subduction zone earthquakes. All of these components are necessary to develop a comprehensive seismic hazard assessment or map that includes contributions from specific local fault sources. However, to date the existing fault mapping of Guam is limited to bedrock geology maps (Tracey *et al*., 1964; Siegrist et al., 2007), Quaternary fault mapping based almost entirely on aerial photograph interpretation (Dames and Moore, 1994), and a recent more detailed and field-checked map of the Tamuning-Yigo fault by URS (Olig *et al*., 2007). Even the location of the faults is not well known, and there is very little information regarding their sense of slip or other basic characteristics. Existing fault maps from Dames and Moore (1994) and EERI (1995) have large differences in fault locations, while Olig *et al*. (2007) found in their investigation of the Tamuning-Yigo fault that the existing fault maps had mislocated the fault by at least half a kilometer in the area they studied. The existing data regarding the age of faulting is limited to recognition that several faults affect marine terraces cut into Plio(?)-Pleistocene limestone, reconnaissance observation of some displacement of probable Holocene terraces (Dames and Moore, 1994), and differential uplift of the Merizo limestone, which may be mid-to-late-Holocene.

3.0 RESULTS

This study was designed to address one of the missing elements for adequate fault characterization, a modern Quaternary fault map. For this study, we have undertaken an aerial photograph, LiDAR and field mapping investigation of the Quaternary faults of Guam and have produced a late Quaternary fault map of the island. Clearly an accurate map of the active faults is a necessary first step in evaluating the seismic hazard of Guam. Information about the timing of fault rupture is also a necessary element to assessing hazard, and our current knowledge of the area suffers from a lack of absolute ages of late Quaternary deposits and geomorphic features. That is a crucial part of developing a complete understanding of fault activity, but it is beyond the scope of this project. However, we have identified and described some potential sites for future detailed study of the paleoseismic characteristics of faults. Similarly, improved characterization of the subduction zone would benefit the assessment of seismic hazard. The presence of numerous marine terraces along the coast of Guam could be used to improve that characterization. That too is beyond the scope of this study, which is restricted to assessment of crustal faulting.

3.1 Methods

Using existing fault maps as a starting point for our investigation, we analyzed a variety of sources to develop a preliminary map. We used this map to guide our field investigations in Guam, which took place over the course of one week in January 2013

The primary data source we used to develop our map was a 1-m resolution digital elevation model (DEM) derived from airborne LiDAR data. Hillshades developed from this DEM form the basemap for the fault map, presented in Plate 1. The LiDAR data were obtained from the National Oceanographic and Atmospheric Administration's Ocean Service, Office for Coastal Management, Joint Airborne Lidar Bathymetry Technical Center of Expertise (JALBTCX) (2007). The dataset included topographic data across the entire island and bathymetric data to a depth of 40 m or laser extinction. The data were obtained in sufficient density to create 2-foot contours, and were classified into return categories using TerraScan. URS developed 1-m resolution bare-earth digital elevation models from the LiDAR data.

In addition to the LiDAR-derived topographic dataset, we also examined:

- DEM of the bathymetry around the island of Guam beyond the extent of the JALBTCX (2007) limits, from the NOAA Center for Tsunami Research, compiled from multibeam data from numerous missions and belnded with JALBTCX (2007) data
- 1993 ≈ 1:26,000 scale black and white stereo aerial photographs covering the entire island of Guam. These photos, currently on loan to URS, will be scanned and reprinted.
- 1992 to 1994 black and white digital orthophotographic quadrangles (DOQs)
- 2001 color IKONUS photography
- Topographic data (7.5' U.S. Geological Survey [USGS] quadrangles with 20 ft contour intervals and digitized 10-ft-contour interval data constructed by Perry and Associates from 1993 photography)

Using the above sources, we developed a preliminary map of lineaments and potentially fault-related geomorphic features. In addition, we developed a catalogue of sites for field checking. This map was compiled in ArcGIS 10.

We also benefitted from the use of data acquired and compiled by Fugro Consultants Inc. (Fugro, 2011) for the Navy Geothermal Program Office. These data included their report as well as numerous GIS files including their reconnaissance fault mapping, Landsat imagery and other publicly available data.

In January 2013, we visited Guam. We traversed the island, across publicly accessible areas, examining all of the major faults and the targeted locations identified in our desk study, in order to field check our office-based mapping, view exposures of the fault, look for indications of age of activity, and identify sites for future in-depth fault investigations. We were not able to gain access to sites on military bases during this visit. However, one of the authors (Zachariasen) visited Guam again in April 2015 and did visit some sites on bases. Some observations from that trip are described here as well.

The results of the field reconnaissance study were used to refine the existing mapping and inform our interpretations. The final map was compiled in GIS and is presented at a scale of 1:50,000 in Plate 1.

3.2 Fault Map

The fault map in Plate 1 shows likely Quaternary faults and lineaments of uncertain provenance but which might be fault-related that were mapped as part of this project. Many of the faults, including the Mt. Santa Rosa, Machanao, Tamuning-Yigo, and Adelup faults were previously identified in the Tracey et al. (1964) bedrock mapping (Figures 2 and 3), but in many cases this study has shown that they are longer or more complex than previously indicated. In addition, we have identified several new faults that are likely Quaternary, including the Ritidian, Anderson Airforc Base (AAFB), Finegayan, and Agana faults. Finally, we have not included some faults from Tracey et. al. (1964), including the Talofofo fault, which shows no evidence of Quaternary activity, and the Cabras and Cocos faults, which we did not recognize as Quaternary faults in the Lidar and which were not field checked; they may be Quaternary, but are not defined so as part of our mapping.

The general distribution of Quaternary faulting shown in Plate 1 indicates that the majority of the faulting is concentrated in the northern part of the island and affects the Mio-Pliocene Barrigada and Plio-Pleistocene Mariana limestones, which form the plateau that encompasses the northern part of the island (Figures 2 and 3). Most of the faults in the northern plateau region strike northwest, with the exception of the northeast-striking Tamuning-Yigo fault.

The Adelup fault forms the boundary between the limestone terrane to the north and the volcanic terrane to the south (Figure 2). The southern, volcanic region differs dramatically from the northern plateau. We mapped a small number of short lineaments in the south, but, with the exception of two short potentially Quaternary scarps on the west and south coasts, we did not identify any significant Quaternary faults or fault-related features. The region is extensively dissected, and the volcanic rocks are readily eroded, in contrast to the resistant limestone plateau in the north, so it is possible that faulting is present in the south at low rates such that the geomorphic expression of faulting is removed by erosion. Nevertheless we saw essentially no indication of active faulting in the entire southern region. This is consistent with previous studies (e.g. Dames and Moore, 1994; Fugro, 2011).

3.3 Fault Characteristics

This section includes descriptions of the mapped faults and lineaments, from north to south, including evidence of faulting from Lidar and field investigations.

3.3.1 Ritidian Fault Zone

On the plateau above Ritidian Point, in the Machanao structural block (Figure 2), a north-northwest-striking fault extends from Ritidian Point in the northwest toward Mt Santa Rosa to the southeast. Tracey et al. (1964) mapped a short vertical joint across the coast at Ritidian Point but did not extend it into the upper plateau. Siegrist et al. (2007) remapped this feature as a fault, but again did not extend it beyond the lower coast (Figure 3). Here, we map a continuous scarp for 10 km from Ritidian Point across Anderson Air Force Base to Salisbury Junction (Plate 1; Figure 4). This scarp generally corresponds with a brecciated zone mapped by Tracey et al. (1964) and Siegrist et al. (2007).

The scarp is up on the southwest through this extent and ranges from 10 to 30 m high (Figure 5). The scarp is pronounced everywhere except through the runway area, where extensive surface modification may have obliterated it. A second scarp runs subparallel to and 1-2 km southwest of the Ritidian scarp. This fault is also down to the northeast, with relief of about 10 m and pronounced southwest slope on the northeastern side of the fault. The Ritidian fault is crossed at nearly right angles by two cross faults. The northwestern fault scarp is down to the southeast, about 6-8 m. Cross-cutting relationships with the Ritidian fault are uncertain; scarps heights of both faults are similar on either side of the intersection (excluding the runway area). The southeastern cross fault truncates the subparallel scarp to the southwest of the Ritidian scarp. It is down to the northwest; scarp heights are markedly different across the Ritidian fault, about 15 m on the southwest side of the intersection and 4 m on the northeast. Scarp heights across the Ritidian fault also differ on either side of the cross fault; to the northwest, profile RF-C shows relief of about 10 m, whereas profile RF-D on the southeast shows a double scarp with about 30 m of relief. The cross fault scarp merges into the Machanao fault to the west and dies out in a broad swale to the east, across another small fault labeled AAFB (Anderson Air Force Base) fault, and within more heavily modified runway areas (Figure 5).

The Ritidian fault may connect with the Mt. Santa Rosa fault (fault name as defined in Dames and Moore, 1994), east of Mt. Santa Rosa, but that relationship is uncertain. Around Salisbury Junction, a scarp continues on strike with the Ritidian fault, but the fault is discontinuous, composed of two traces, and the polarity changes, with northeast side up (Figure 5). The Mt. Santa Rosa fault as previously mapped (e.g. Tracey et al., 1964; Dames and Moore, 1994) is again reflected as southwest-side-up scarps (Plate 1). This long zone likely represents the same structure, but the changing polarity suggests a steep fault dip and perhaps a component of strike slip. The fault may also extend offshore. Numerous north-striking scarps and lineaments are evident in the bathymetry along strike of the Ritidian fault north of Ritidian Point. No scarps appear to traverse the shelf between the offshore scarps and the onshore Ritidian fault, but nearshore process may obliterate evidence of faulting. If all the on-strike scarps represent a single fault zone, its onshore length is about 16 km; including the mapped offshore traces increases the length to about 23 km, and it could, of course extend farther beyond the mapped area.

Most of the Ritidian fault lies in military areas and has limited field accessibility. However, access to two locations reveals evidence for likely Holocene activity (Sites R1 and R2 in Figure 4). Figure 6a shows photographs of a small (ca. 0.5-1 m) scarp in limestone on the larger scarp, which may represent a Holocene scarp (Site R1). A roadcut in the scarp exposed the fault plane, underlying a small break in slope and scarp that was discontinuously present along the larger scarp (Figure 6b). The fault in this exposire dips steeply west, indicating reverse movement, although the faults in Guam have generally considered to be normal faults. Again, a component of strike-slip is suggested.

The northern end of the onshore fault corresponds with the northern edge of a deep scalloped paleo-embayment that contains a well-preserved flight of marine terraces (Figure 7). The fault is not evident through this area likely due to extensive landsliding. Siegrist et al. (2007) do map a fault to the east of the scalloped area, but it is not evident topographically and the fault as mapped here runs into the eastern edge of the scallop. Dames and Moore (1994) used flight set of marine terraces to infer an uplift rate for northern Guam. They interpreted the highest terrace to represent either MIS-5e or MIS-5c. We are not determining uplift rates here, but we can use the marine terraces to assess displacement across the fault. Figure 8 shows two topographic profiles across the terraces on either side of the fault (locations in Figures 5 and 7). The profiles indicate that older terraces are progressively higher on the south side of the fault than the north side, suggesting continued faulting throughout the period of terrace formation. We can use the terrace elevation differences with inferred ages based on global sea-level curves and other data to infer vertical displacement rates on the fault (Table 1). We use Dames and Moore's (1994) terrace identification for some rate calculations, although the location of the MIS 5e Tarague Limestone suggests they may be in error, as noted earlier, with terrace ages underestimated. Rates using Dames and Moore (1994) dates thus should be considered maximums, whereas the rates using the age of the Mariana limestone is likely a minimum.

Table 1. Estimated slip rates on the Ritidian fault

Terrace	Elevation Difference (m)	Age	Vertical displacement rate (mm/yr)	Note
1	1.0 ± 0.5	3-5 ka	0.1 - 0.5	Age estimate assumes terrace marks mid-Holocene highstand
2	5.0 ± 1.0	40 ka 59 ka	0.1 - 0.15 0.07 - 0.1	Age estimates from Dames and Moore (1994) correlation to MIS stages, either 3a (40 ka) or 3d (59 ka)
3	14 ± 5	59 ka 96 ka	0.15 - 0.32 0.09 - 0.20	Age estimates from Dames and Moore (1994) correlation to MIS stages, either 3d (59 ka) or 5b (96 ka)
Plateau surface	~14	1.8 - 2.0 Ma	0.007 - 0.008	Age estimate from assuming age of plateau surface is age of Mariana Limestone deposition, ca 1.8 - 2.0 Ma. Minimum rate estimate.

3.3.2 Anderson Air Force Base Fault

The Anderson Air Force Base (AAFB) fault is a short (ca. 8 km, onshore), northwest-striking fault that lies northeast of and parallel to the Ritidian fault (Plate 1 and Figure 4). It may be part of the same system, and it strikes toward Mt. Santa Rosa as the Ritidian fault does. This fault has not been depicted in published maps previously, but is reflected in a northeast-side-up scarp cutting across the northeast runway area of Anderson Air Force base. We did not examine this fault in the field, so all characterization is based on remote geomorphic assessment.

The AAFB scarp is steep and has about 10 m of relief south of the northeast-striking fault that crosses this and the Ritidian fault (Figure 9). North of this cross fault the scarp is degraded and poorly expressed on the plateau; the area around the downthrown side of the fault is characterized by sinkholes, closed depressions, and others indicators of karst topography. The ridge that marks the edge of the plateau to the north, however, shows a well-defined step up to the east across the fault. The fault also appears to affect the flight of marine terraces cut into the cliff along the northern coast (Figure 10). It manifests as a distinct lineament through the upper levels of terrace but is not clear across the lowest terraces. Topographic profiles of the terraces on either side of the fault suggest some east-side-up displacement (Figure 11). The elevation of the top of the ridge on the plateau is as high as 30 m; however, the plateau surface behind the ridge has an elevation difference of closer to 10 m. The profiles indicate a fair amount of denudation of the plateau surface since its abandonment. Nevertheless, the profiles suggest, though not as strongly as those at Ritidian Point, that successive displacements occurred on this fault over the time the terrace surfaces were cut, as the younger terraces appear to be offset less than the older ones. There is no clear evidence of elevation difference of the lowest emerged surface, which is presumably associated with the mid-Holocene highstand, suggesting that this fault has not ruptured since that time (ca. 3000-5000 BP).

3.3.3 Machanao fault

A northwest-striking fault lies subparallel to and about two km southwest of the Ritidian fault. It strikes into the faults that bound the southwest edge of Mt. Santa Rosa (Figure 12 and Plate 1). We call this fault the Machanao fault after Dames and Moore (1994). The western part of the fault has a well-defined northeast-side up scarp, about 15 m high (Figure 13). Along Mt. Santa Rosa, the east side is also up, and the fault is marked by a series of saddles along the flank of the mountain, where erosion and landsliding have obscured it somewhat. Southeast of Mt. Santa Rosa, the fault crosses the limestone plateau and forms an east-side-up scarp about 10 m high. The fault is still evident topographically as it crosses the cliff and a series of marine terraces (Figure 14).

In the western section of the fault, the scarp parallels a road behind houses set at the base of the scarp (Site M1). A small step, ca. 0.5 m high and easily obscured in the jungle underbrush, traverses the foot of the main escarpment (Figure 15a). It is marked by an accumulation of limestone cobbles, and the slope of the scarp above this feature is somewhat steeper than that below. We interpret this step to represent the most recent displacement on the fault and judge that it is likely Holocene in age.

Where the fault traverses the western edge of Mt. Santa Rosa, it is expressed by a series of saddles along the southwest flank of the mountain. At the west side of Mt. Santa Rosa, a quarry reveals numerous faults exposed in the Tertiary Alutom formation (Site M2). The beds of the Alutom formation dip 35 -45˚ to the southwest. An angular unconformity marks the contact between these beds and overlying alluvium derived from the Alutom. Faulting exposed within the Alutom does not appear to offset the unconformity or the overlying alluvium (Figure 15b). Faulting here, however, is off the main scarp that marks the Quaternary fault extending toward the center of the island.

Where the fault crosses the marine terraces, topographic profiles of the terraces on either side of the fault reflect the north-side-up displacement (Figure 16). The terraces are not very well defined and have been differentially preserved. The flight of terraces shows the elevation of uppermost platform is approximately 20 m higher on the north side, consistent with the 15-m scarp observed there. The inset marine terraces appear, in general, to have successively decreasing amounts of relative elevation difference the lower, and younger, they are, but correlations are uncertain in places, leading to some uncertainty in determining the elevation differences. The terrace profiles do suggest, however, that, depending on the correlation, the two lower terraces (near the modern coastline at ca. 2 m elevation and at about 20-30 m elevation) may have the same amount of elevation difference (2m), suggesting there was no displacement on the fault between the cutting of the two surfaces. Although the age of these terraces is not known, the older terrace is likely at least tens of thousands of years old (at Ritidian Point, Dames and Moore [1994] inferred terraces at ca. 24 m were 40-59 kyr, and other interpretations [e.g. Randall and Siegrist, 1996] would have it greater than 100 kyr), suggesting a recurrence interval of tens of thousands of years. Conversely, if the alternative correlation holds true, the terrace on the north side is 4-5 times higher than its correlative on the south side, and likely several events have occurred on the fault since the formation of the higher terrace.

The scarp is evident crossing the lower terrace surfaces, coastward of the steep cliffs and older terraces. Topographic profiles across the fault on two of these lower surfaces, at about 20 and 25 m elevation, indicate that offset on both is the same, about 2 m and that no event occurred between the formation of the two surfaces.

3.3.4 Finegayan Fault

We did not visit this fault in the field. Its geomorphic expression in the Lidar, however, suggest it has not moved in the latest Quaternary (Figures 12 and 13). The fault is high, but subdued, modified by karst geomorphology. We have not recognized any smaller scarps, suggestive of recent movement.

3.3.5 Tamuning-Yigo Fault

The Tamuning-Yigo fault is distinctive from other late Quaternary faults on Guam because of two characteristics: 1) it is the longest fault on the island; and 2) it is the only major fault that strikes east-northeast. It extends at least from Agana Bay on the west to Mt. Santa Rosa on the east, a distance of about 18 km. It may continue along the west coast of Guam, along the shoreline, where it is difficult to discern if the steep escarpment is a fault scarp or a sea cliff, as far as Orote Point and offshore, or it may be truncated by the Adelup fault (Plate 1). It may also extend offshore to the northeast, or conversely be cut off by the northwest-striking faults such as the Machanao, AAFB, and Ritidian faults.

The Tamuning-Yigo fault is characterized by fairly continuous down-to-the-north scarps (Plate 1 and Figures 17 and 18). These fault scarps offset Plio-Pleistocene Mariana limestone (units QTmr and QTmd of Tracey et al., 1964 and Siegrist et al, 2007) and younger, late Quaternary(?) marine terraces cut into the Mariana Limestone (Figure 3). In the central and northeast sections of the fault, it also offsets Mio-Pliocene Barrigada limestone (unit Tbl).

A steep, prominent northeast-trending scarp that is 30 to 45 m high extends from Agana Bay, along the northwestern edge of the Guam International Airport, to Highway 16 (Figures 17 and 19). At its western end where it intersects Marine Drive, this fault scarp appears to have been eroded into during formation of a younger marine terrace. Topographic profiles of the coast on either side of the fault indicate that the elevation of this terrace is about 2.5 m above sea level on the north and south sides of the scarp. If this terrace correlates to the Merizo Limestone, it suggests that movement on the Tamuning-Yigo fault is older than 2750 to 4350 BP, the age of the limestone. Although a cliff of Mariana limestone is partially exposed at this intersection, no fault exposure is evident, but vegetation obscures the top of the exposure, and development has extensively modified the base of the cliff. The main scarp of the Tamuning-Yigo fault that extends along the airport is surprisingly steep and has a paucity of colluvial deposits at its base, which is somewhat unusual on the downthrown side of a normal fault scarp. These characteristics, along with the scarp's linear geometry suggest that the fault is steeply dipping to near vertical, and may have a strike-slip component of slip. In contrast, east of Highway 16, the fault scarp changes to a more easterly strike. It also becomes broader and more arcuate, curving toward the downthrown side (Figure 17). These characteristics are more typical of normal-slip faults.

In the central section of the fault, west of Mogfog, we observed the fault exposed in a quarry wall (Site TY1, Figure 20a). It was moderately to steeply north-dipping, and a small break in slope was visible in the slope above the fault, but no late Quaternary deposits overlay it to reveal age relationships. Near Mogfog, a series of landslides have modified and obscured the main escarpment (Figure 17). Here, short, discontinuous, arcuate north-facing scarps are head scarps of coalescing slumps that have cut into the upthrown side of the Tamuning-Yigo fault and modified the scarp. Crosscutting relations are not always clear, but some, if not all, of the slope movement on landslides appears younger than faulting or may have been triggered during earthquakes either on or off the Tamuning-Yigo fault. The scarp is high, but laid back; we did not see evidence of a Holocene scarp (Figure 20b). At Mogfog, a south-side-down scarp parallels the main Tamuning-Yigo scarp, about a kilometer to the north (Figures 17 and 18; TY3). Although possibly modified by fluvial processes, this is likely an antithetic fault to the Tamunig-Yigo fault.

East of Mogfog, Tracey et al. (1964) and Siegrist et al. (2007) show the fault changing polarity from down-to-the-north to down-to-the-south (Figure 3). However, this is not consistent with the topographic expression and our observations of the main Tamuning-Yigo fault near Mogfog.

Based on our interpretation of LiDAR data and our field reconnaissance, the Tamuning-Yigo fault is characterized by down-to-the-north fault scarps both east and west of Mogfog. A few kilometers northeast of Mogfog, the main trace of the Tamuning-Yigo fault is again evident as a prominent down-to-the-northwest scarp that bifurcates into two scarps. These down-to-the-northwest scarps are in the same area where Tracey et al. (1964) and Siegrist et al. (2007) map older (Miocene to Pliocene) Alifan (Tal) and Barrigada (Tbl) limestone on the north (downthrown) side of the Tamuning-Yigo fault, whereas younger (Plio-Pleistocene) Mariana Limestone (QTmr and QTmd) are shown on the south (upthrown) side of the fault. This suggests that the Tamuning-Yigo fault actually shows reverse or reverse-oblique slip along this portion of the fault, with younger rocks pushed up and over older rocks. Reverse-oblique slip on a north-northeast-striking fault would actually be more consistent with the northwest-directed compression expected along this convergent plate boundary.

In the northeast section, the Tamuning-Yigo comprises two primary down-to-the-west scarps, but includes numerous smaller scarps and traces, both east and west side up. Near Lumuna, the more prominent trace changes from the eastern, upper trace to the western, lower and the eastern scarp becomes ill defined. At Site TY4, it is exposed in a quarry and appears as a subvertical zone of shearing (Figure 20c). The faulting extends to the surface, but there are no younger deposits overlying it. In general, the Tamuning-Yigo fault, while a large scarp with a fair amount of cumulative slip, appears less active than the faults to the north. At its northeast end, the Tamuning-Yigo fault has a complex relationship with the faults around Mt. Santa Rosa. The fault appears to be cut off by the Machanao fault, although a fault on strike with the eastern trace of the Tamuning-Yigo fault continues past the Machanao and Mt. Santa Rosa faults which may be part of the Tamuning-Yigo system.

In summary, the Tamuning-Yigo fault shows evidence that suggests a variety of slip directions that appear to change along strike and include normal, oblique and reverse slip. Although this needs further investigation to be better documented and understood, this complexity is not surprising given the complex stress patterns due to multiple plate interactions in the region. For example, one possibility is that the Tamuning-Yigo fault was originally an old transform fault that has been reactivated, perhaps only partially, during late Quaternary uplift of Guam. This could explain why the Tamuning-Yigo fault shows evidence for repeated late Quaternary activity along some portions, but still appears to be older than northwest-striking faults at both of its ends. Reactivation may also explain some of complexities in geometry and slip directions. Regardless, the geologic evidence indicates that the Tamuning-Yigo fault has been repeatedly active during the late Quaternary (past 130,000 years), whereas movement is likely older than late Holocene (3,000 to 5,000 years), it still should be considered a potential earthquake source and surface faulting hazard on Guam.

3.3.6 Agana Fault

The Agana fault is a newly identified fault that extends at least 5 km from Agana Bay to Sabana Maagas (Figure 21). It may be longer, extending offshore on the west, or extending eastward from Sabana Maagas through Mangilao. If it does extend feather eastward, it does not have a scarp associated with it, and we did not identify an extension in the LiDAR. It lies about 2.7 km south of the Tamuning-Yigo fault, parallel to and about 2 km north of the Adelup fault. The fault manifests as a south-side-up scarp running along the north edge of the communities of Agana Heights and Sinjana (Figure 22). The upthrown side forms a broad plateau occupied by the residential area of Agana Heights and the US Naval hospital; the downthrown side is occupied by the Agana Swamp. Scarp height decreases from about 60 m on the west to 30 m near the east end until tapering to nothing eastward (Figures 21 and 22).

3.3.7 Adelup fault

The Adelup fault is one of the largest faults on the island and forms the boundary between the northern limestone plateau and the southern dissected volcanic terrane (Figures 2 and 3). It is a south-side-up normal fault that extend from Adelup on the west coast to Pago Bay on the east, traversing the hills of on the west side of the island and the running along the southern edge of the Pago River floodplain on the east (Figure 21). A series of topographic profiles illustrates the fault morphology along strike (Figure 22).

The Adelup fault comprises a broad zone encompassing several subparallel fault races at the eastern end. The northern trace runs along a scarp at the coast behind the Pacific War Museum (Site A1, Figure 21). The westernmost section of this trace appears cut into during formation of a marine terrace. The broad terrace surface that extends right to the scarp is heavily modified, but appears not to be the lowest, Merizo, terrace but a few meters higher (Figure 22b, profile AF-6). Modification of the surface makes it difficult to see the relationship between this terrace surface and faulting.

Eastward, where the fault crosses the Fonte River, the fault comprises three traces (Figure 21). The northernmost passes through a saddle northwest of the Fonte River; no young scarp is evident across this saddle. The middle trace, however, follows a >1-m-high scarp that appears in debris flow material near the base of a 2-m high limestone scarp (Site A2l, Figure 21; Figure 22b, profile 5a). We interpret this scarp to represent a latest Quaternary/Holocene scarp.

To the east, the fault crosses the Pago River. It is not evident in the LiDAR as a topographic scarp across the floodplain (Site A3, Figure 21; Figure 22a, profiles 3a-3c). Above the river, to the west, bedded west-dipping volcaniclastics (bedding 172˚/48˚W) contain nearly vertical, steeply dipping ENE-striking mineralized shears (Figure 23a). Although topographic profiles indicate there is no scarp crossing the Pago River recent deposits, we observed a ca. 1-m high scarp, trending about 295˚-300˚, on Holocene terrace deposits of the Pago River (Site A4, Figures 21 and 23b).

At the east end of the fault, at Pago Bay, the fault is exposed in bedrock and observed to displace Holocene marine terraces on Pago Point (Sites A5 and A6, Figure 21). At site A5, homesites at Pago Bay resort have been cut back into the Adelup scarp. We observed the fault in bedrock, striking across the site (Figure 24a), oriented 280˚/85˚N. It extended across the homesites and into the scarp.

On Pago Point, accessible only at low tide, offset of two marine sea-level notche indicates that the fault has had Holocene displacement (Site A6, Figure 21). Sea-level notches form from bio- and mechanical erosion at about mean sea-level to low water. When the land is emergent, the old notches are preserved as records of paleo-sea-level. On Pago Point, a double notch has formed, one modern and one older. Figure 25 shows the notches and their offset across the Adelup fault. The modern notch, which has been forming at about the current elevation since sea-level stabilized after decreasing from the mid-Holocene (ca. 3-5 ka) highstand, about 3,000 years ago, has been faulted. The south is displaced about 80 cm above the modern notch. This indicates that the Adelup fault has sustained at least 80 cm of uplift since the end of the mid-Holocene highstand, ca 2750-4750 BP. Additionally, the older, high paleo-notch, located about 2.5 m above the modern notch, is offset 2.4-3.1 m across the fault, indicating that multiple events have occurred since that notch was formed.

4.0 DISCUSSION

The Lidar data, coupled with field reconnaissance, has allowed us to identify and map several Quaternary faults on the island of Guam. We here use these data to present some preliminary source characteristics for the main Guam Quaternary faults.

Table 2. Source characteristics of Quaternary faults in Guam

Fault	Length	Slip sense	Dip	Age of most recent activity	Slip rate/recurrence
Ritidian	12-20+	N or R	80 SW?	Holocene	0.007 - 0.5 mm/yr
AAFB	8	N?	?	Late Quaternary	?
Machanao	7-16+	N?	?	Holocene	> 0.05
Tamuning-Yigo	18+	N, R, and NO	70-90 N?	<130,000 yrs, probably > 3,000 yrs	?
Agana	6	N?	?	?	?
Adelup	12+	N	70-90 N	Holocene	>0.3 mm/yr; 1 event in ca 3000 yrs

5.0 CONCLUSIONS

We mapped numerous Quaternary faults and lineaments on Guam, using Lidar and field reconnaissance. Previously mapped faults were mapped with greater precision, and additional faults were added. WE have obtained some preliminary data for characterizing these faults. Notably, three faults show evidence of Holocene activity. Further work is required to fully assess these faults and their contribution to the seismic hazard of Guam.

6.0 REFERENCES

Chamberlin, C., 2008. A digital elevation model of Guam for tsunami inundation modeling, NOAA Pacific Marine Environmental Laboratory technical report, Seattle, WA, 7 pp.

Dames & Moore, 1994, Earthquake hazard vulnerability study of Guam, Mariana Islands: Government of Guam, Civil Defense/Emergency Services Office, Agana, Guam, 41 p., Appendices and maps.

EERI, 1995, Guam earthquake of August 8, 1993 reconnaissance report. Earthquake Spectra. Journal of the Earthquake Engineering Research Institute, Supplement B to Volume 11. Craig Comartin, Technical Editor.

Eguchi, T., 1984, Seismotectonics around the Mariana Trough: Tectonophysics, v. 102, p. 33-52.

Hussong, D.M., and Uyeda, S., 1981, Tectonic processes and the history of the Mariana arc: A synthesis of the results of deep sea drilling, in Initial Reports of the Deep Sea Drilling, Project log 60.

Joint Airborne Lidar Bathymetry Technical Center of Expertise (JALBTCX), 2007, 2007 Joint Airborne Lidar Bathymetry Technical Center of Expertise (JALBTCX) Topobathy Lidar: Guam, http://coast.noaa.gov/dataviewer/index.html?action=advsearch&qType=in&qFld=ID&qVal=551

Karig, D.E., and Rankin, B., 19834, Marine geology of the forearc region, southern Mariana Island Arc, in *The Tectonic and Geologic Evolution of Southeast Asian Seas and Islands Part 2*, ed. D.E. Hayes, Geophys. Monograph Series 27: 266-280. Washington DC: American Geophysical Union.

Miklavic, B., 2011, Formation of geomorphic features as a response to sea-level change at Ritidian Point, Guam, Mariana, MS Thesis, Mississippi Sate University, 218p.

Randall, R.H. and Siegrist, H.G., Jr., 1996, The legacy of Tarague embayment and its inhabitants, Andersen AFB, Guam, Vol. III: Geology, beaches and coral reefs: prepared for 36CES/CEV, Unit 14007, Environmental Flight, Andersen Air Force Base, Guam, by Intern. Archaeol., Inc., Honolulu, 461 p.

Rankin, B., Cardwell, R.K., and Karig, D.E., 1984, Kinematics of the Philippine Sea plate: Tectonics, v. 3, p. 555-575.

Siegrist, H.G., Jr., Lewis, R.R., and Jocson, J.M.U., 1998, Seismic hazard vulnerability on Guam: Summary report prepared for Water and Energy Research Institute of the Western Pacific, University of Guam.

Siegrist, H. G., Jr., M. K. Reagan, R. H. Randall, and J. W. Jenson. 2007. Geologic map and sections of Guam, Mariana Islands. Water and Environmental Research Institute, University of Guam, Mangilao, Guam. http://www.weriguam.org/pdf/geologic-maps/map-ofguam.pdf.

Somerville, P., 2000, Earthquake ground motion at the site of the Royal Palm Resort during the August 8, 1993 Guam Earthquake, unpublished report prepared by URS Corporation.

Tracey, J.I., Schlanger, S.O., Stark, J.T., Doan, D.B., and May, H.G., 1964, General geology of Guam: U.S. Geological Survey Professional Paper 403-A, 102 p., plates and maps.

Olig, S., Hemphill-Haley, M., Wright, D., and Terra, F., 2007, Evaluation of potential surface faulting hazards at Guam Memorial Hospital, Tamuning, Guam, URS Corporation unpublished report prepared for Guam Memorial Hospital Authority.

URS Corporation, 2005, Guam hazard mitigation plan: prepared for Government of Guam, Office of Civil Defense.

USGS, 2004, Significant earthquakes of the world: U.S. Geological Survey, Earthquake Hazards Program, accessed in August, http://neic.usgs.gov/neis/eqlists/significant.html.

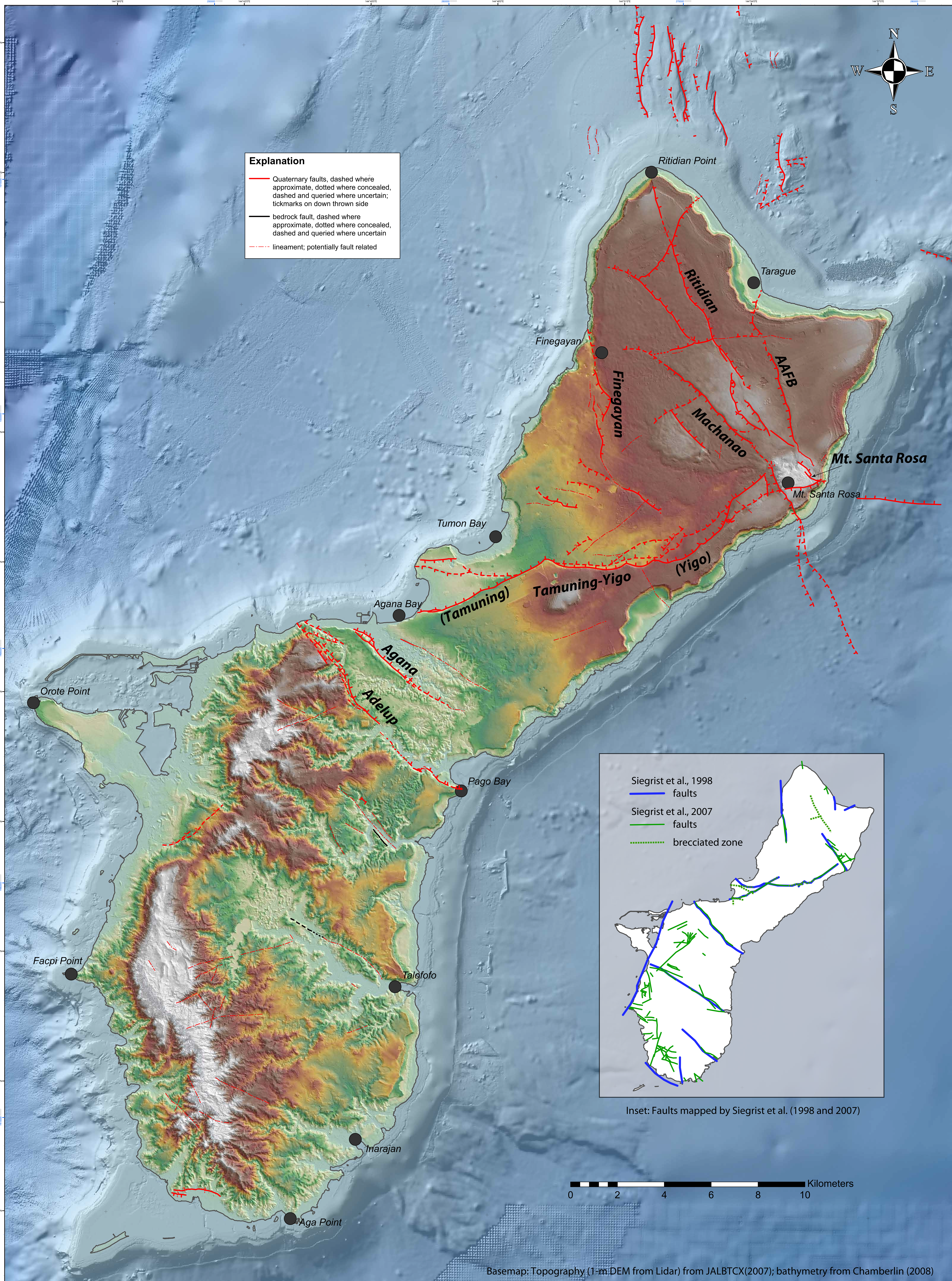

URS

Project No. 26818155

Fault Mapping in Guam

MAP OF QUATERNARY FAULTS AND LINEAMENTS IN GUAM

Plate 1

A.

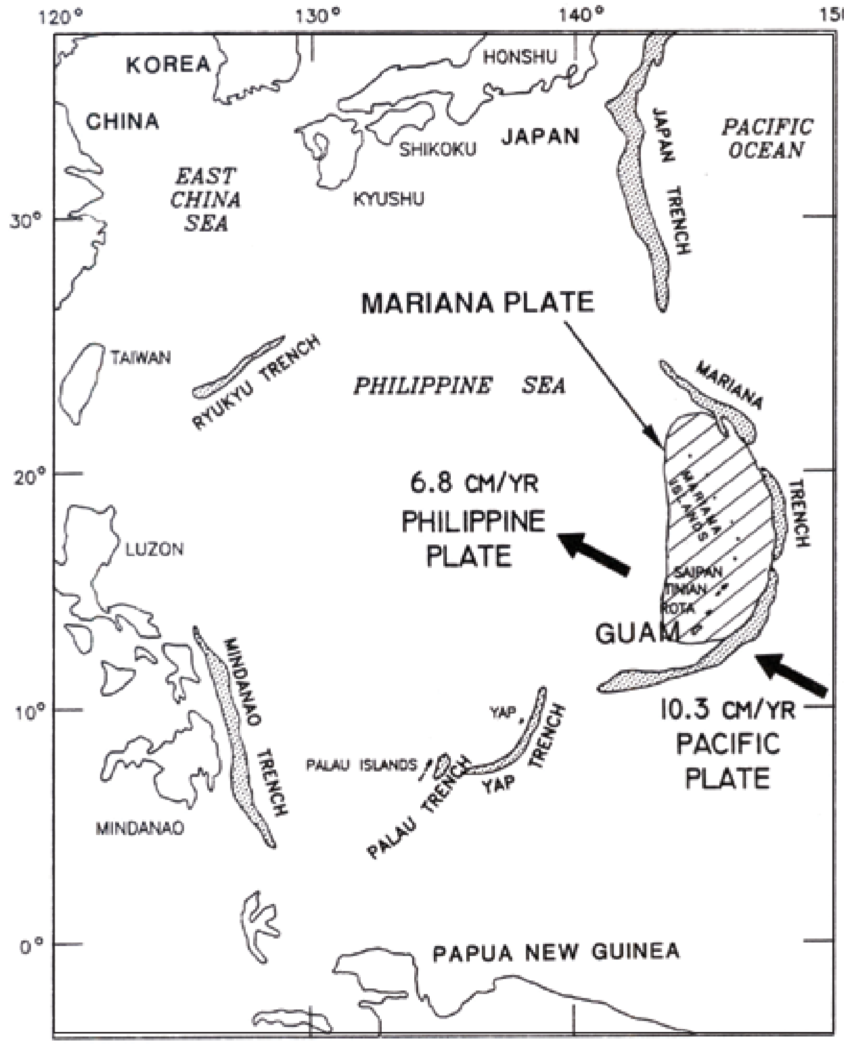

B.

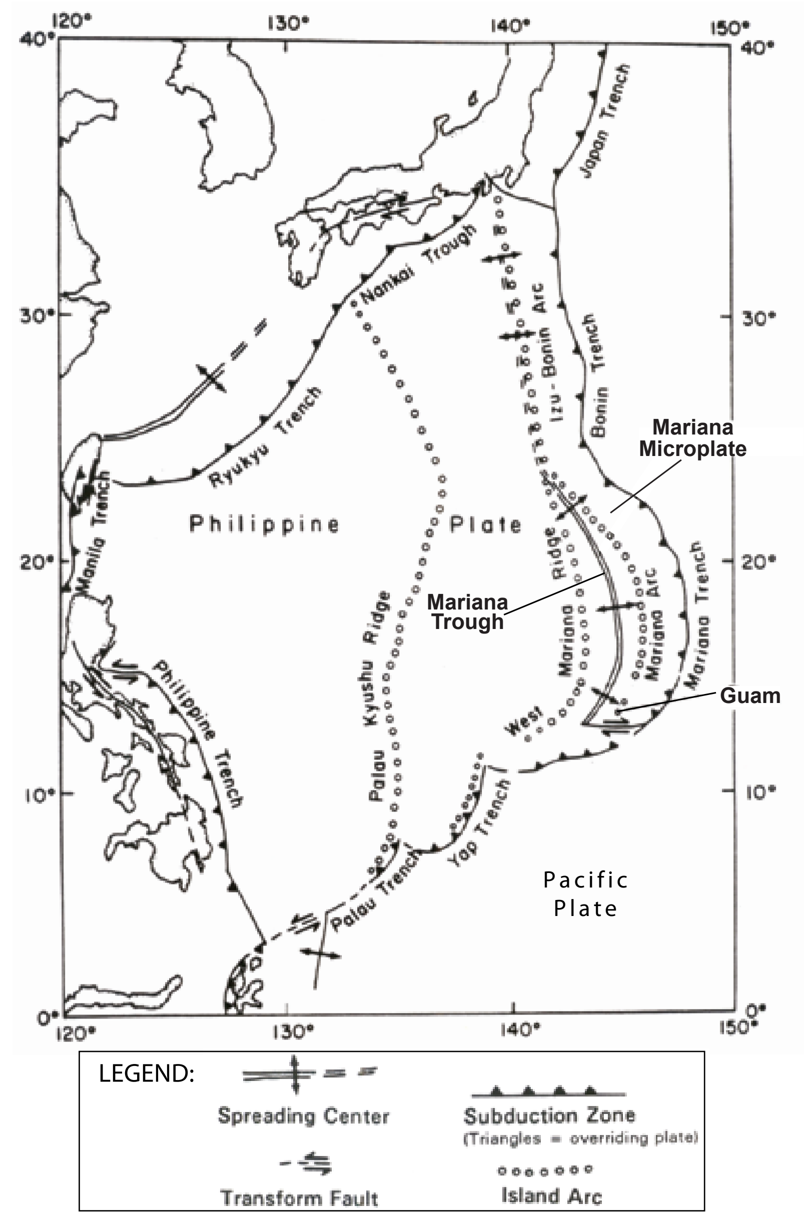

Source: A. EERI (1995).
B, modified from Dames and Moore, 1994, after Karig and Ranken, 1983)

URS	Project No. 26818155	LOCATION MAP AND TECTONIC SETTING OF GUAM	Figure 1
	Fault Mapping in Guam		

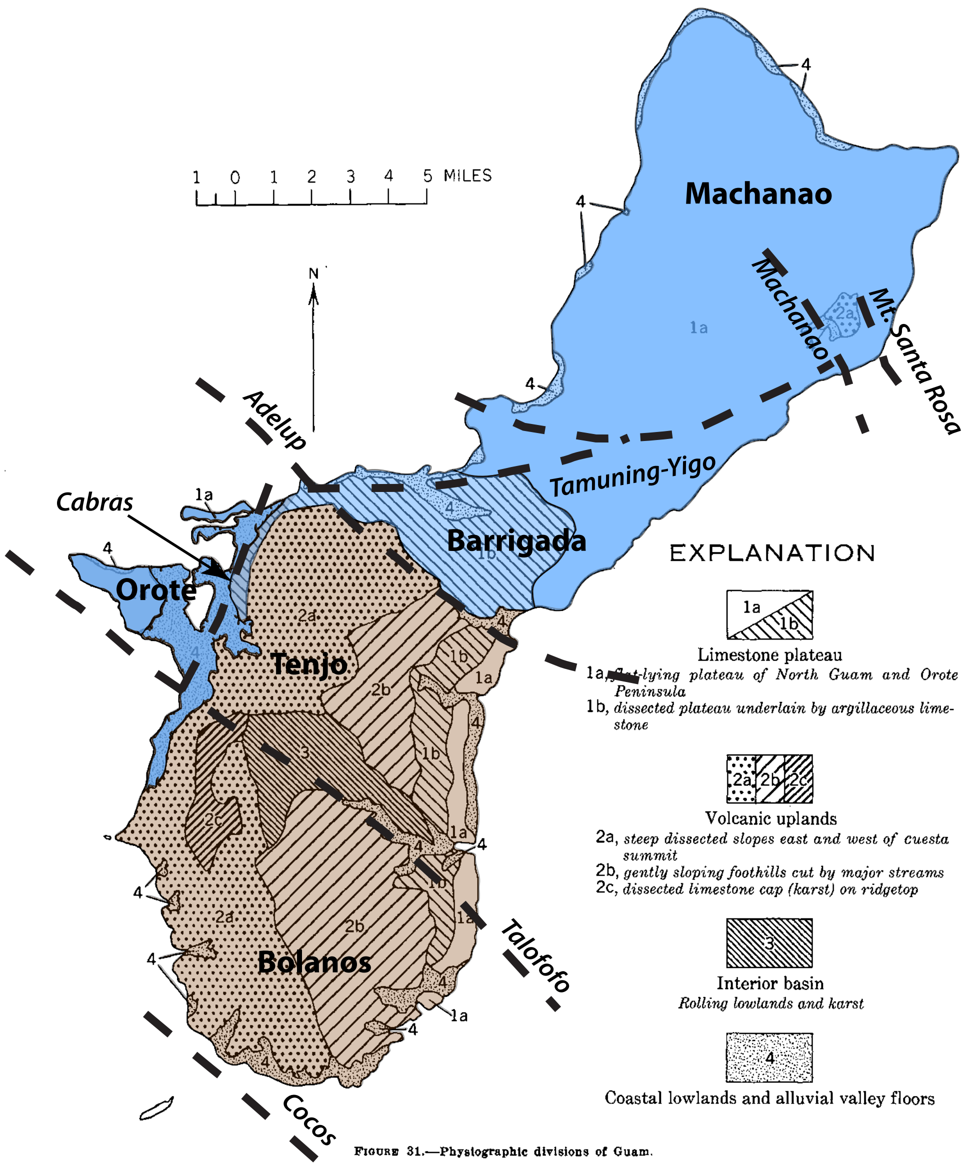

FIGURE 31.—Physiographic divisions of Guam.

Limestone Terrane

Volcanic Terrane

Bedrock faults

Structural blocks labeled in bold

Source: After Tracey et al. (1964)

URS	Project No. 26818155	PHYSIOGRAPHIC PROVINCES, STRUCTURAL BLOCKS, AND BEDROCK FAULTS	Figure 2
	Fault Mapping in Guam		

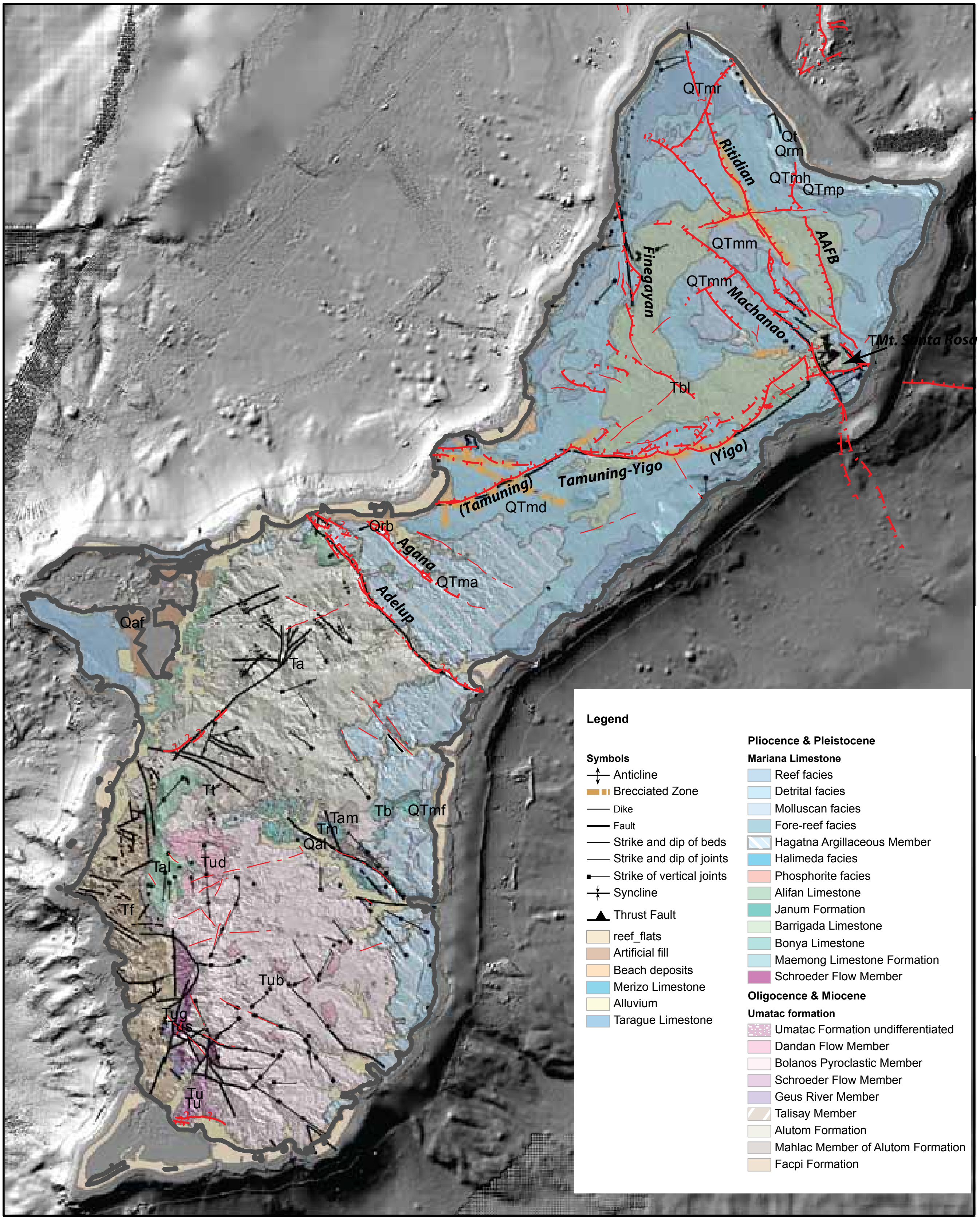

URS	Project No. 26818155	QUATERNARY FAULT MAP (THIS STUDY) OVER GEOLOGICAL MAP (SIEGRIST ET AL., 2007)	Figure 3
	Fault Mapping in Guam		

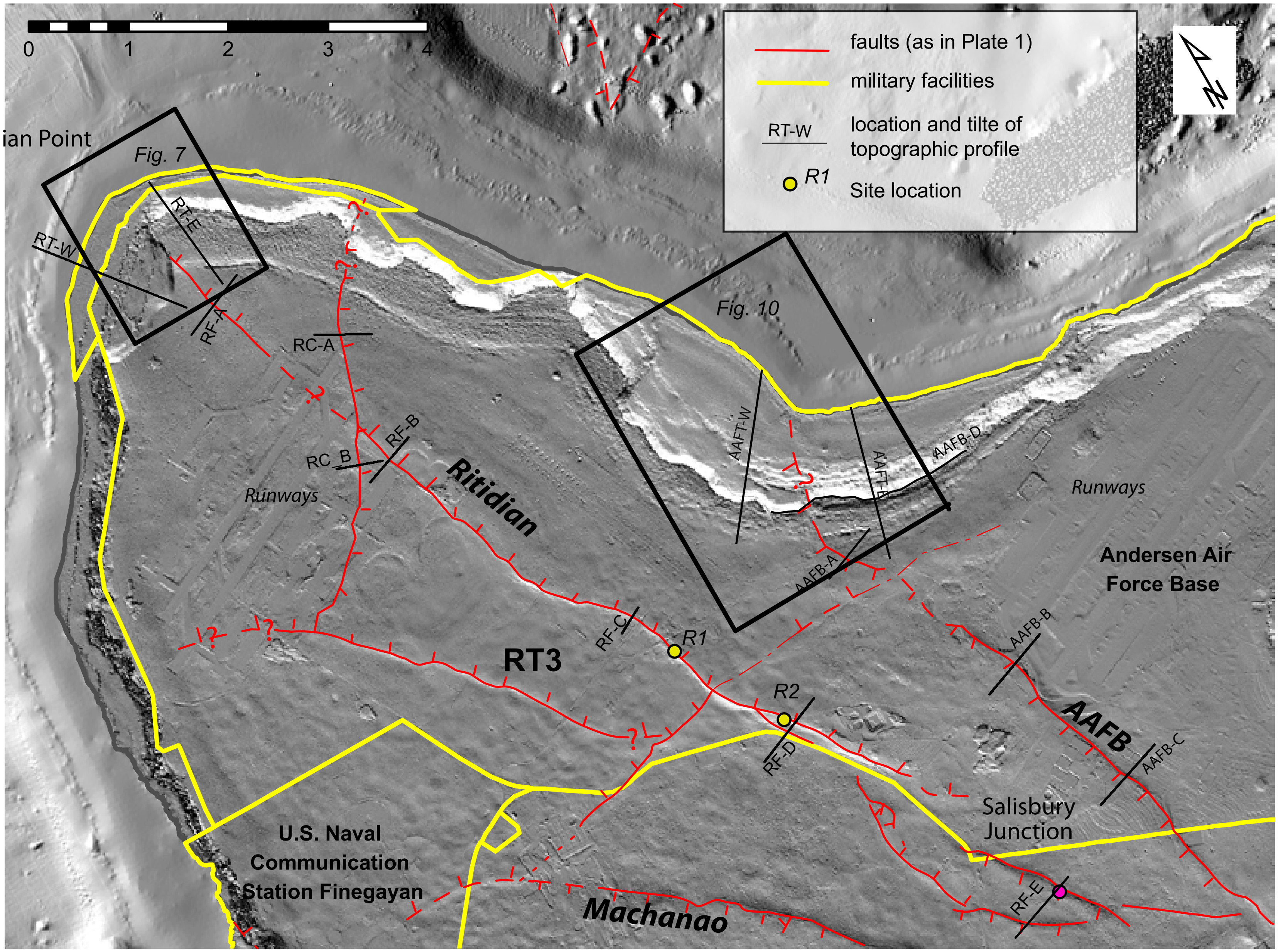

URS	Project No. 26818155	MAP OF RITIDIAN AND AAFB FAULTS NORTHERN GUAM	Figure 4
	Fault Mapping in Guam		

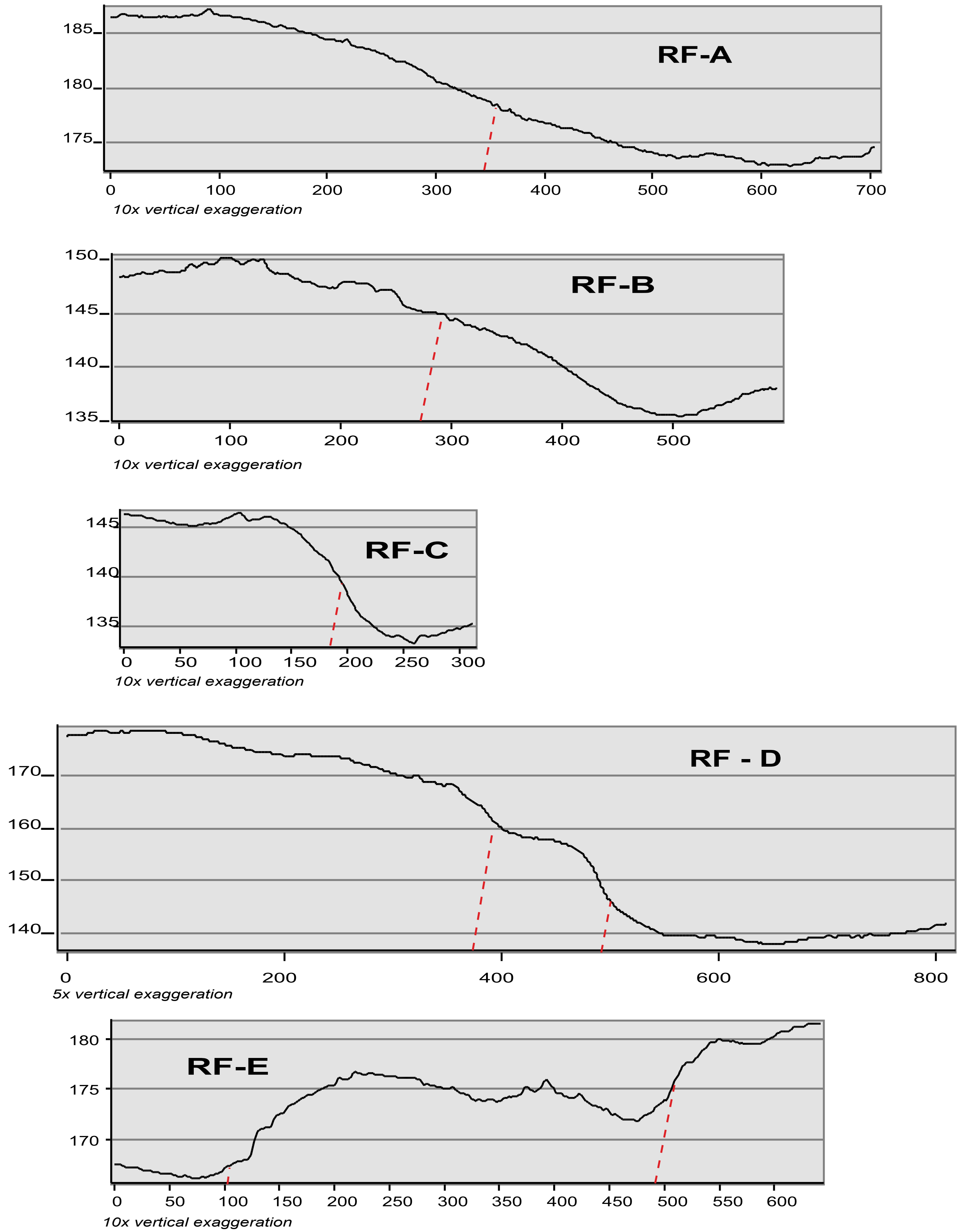

View Northeast

URS	Project No. 26818155 Fault Mapping in Guam	TOPOGRAPHIC PROFILES ACROSS THE RITIDIAN FAULT, NORTHERN GUAM	Figure 5

A.

Small (0.5-1.0 m) scarp in limestone on Rtidian fault scarp at site R1

B.

Scarp exposure at site R2Site R2

URS	Project No. 26818155 Fault Mapping in Guam	PHOTOS OF RITIDIAN FAULT	Figure 6

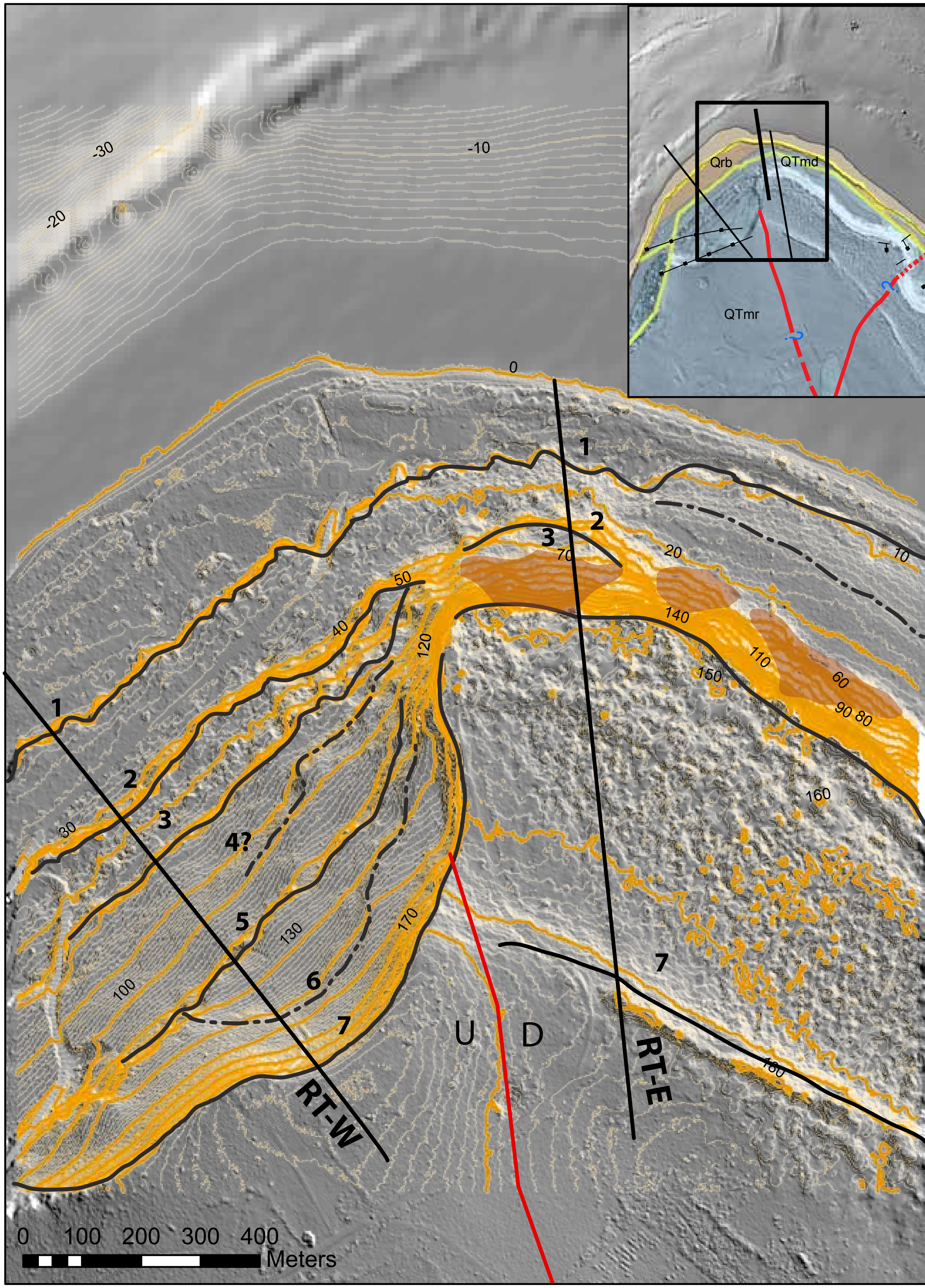

URS	Project No. 26818155	MARINE TERRACES DISPLACED BY RITIDIAN FAULT AT RITIDIAN POINT	Figure 7
	Fault Mapping in Guam		

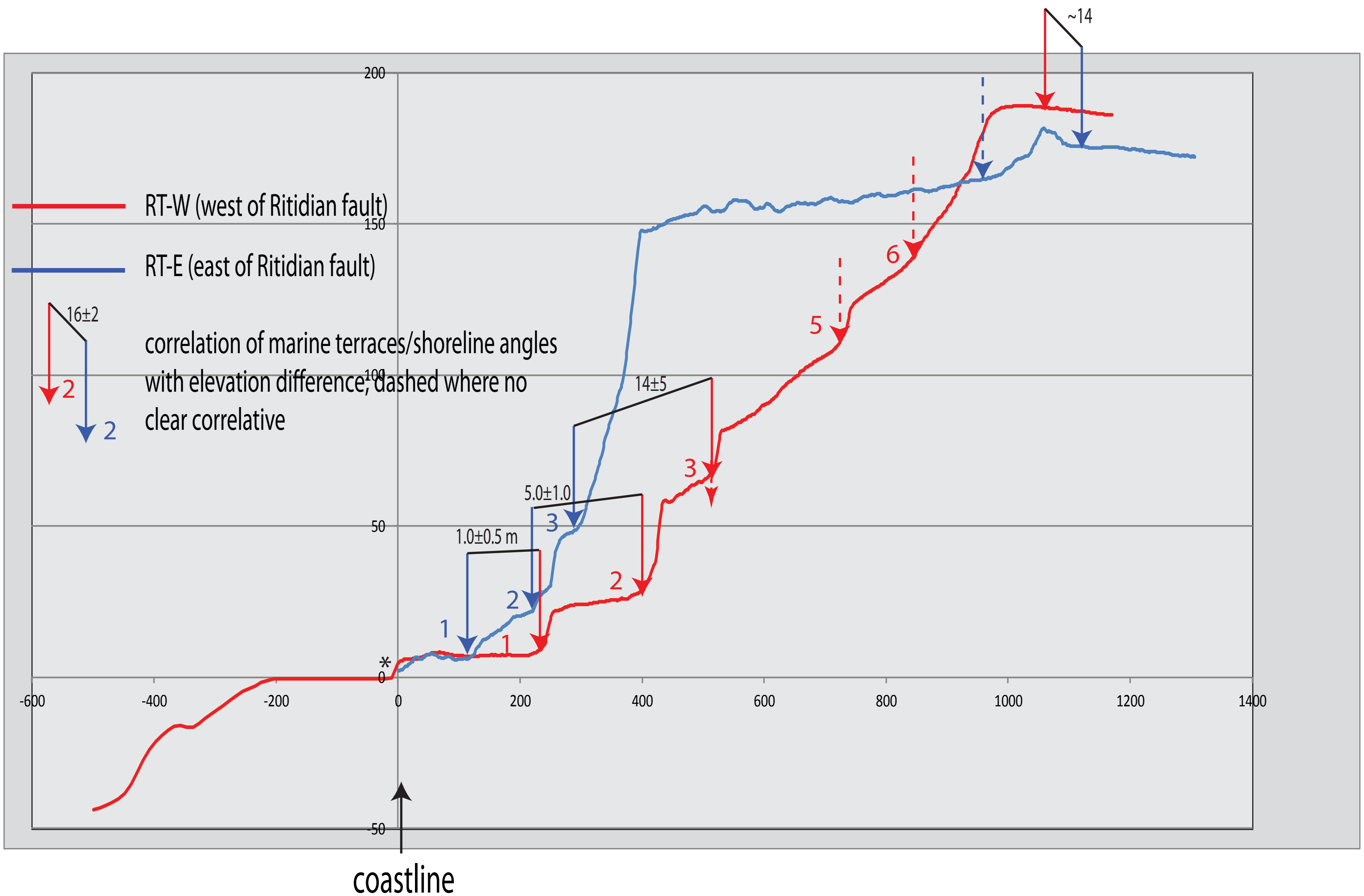

*Apparent step at 0 is artifact of change in dataset from onshore to offshore with ~4m change in datum

URS	Project No. 26818155 Fault Mapping in Guam	TOPOGRAPHIC PROFILES OF MARINE TERRACES AT RITIDIAN POINT	Figure 8

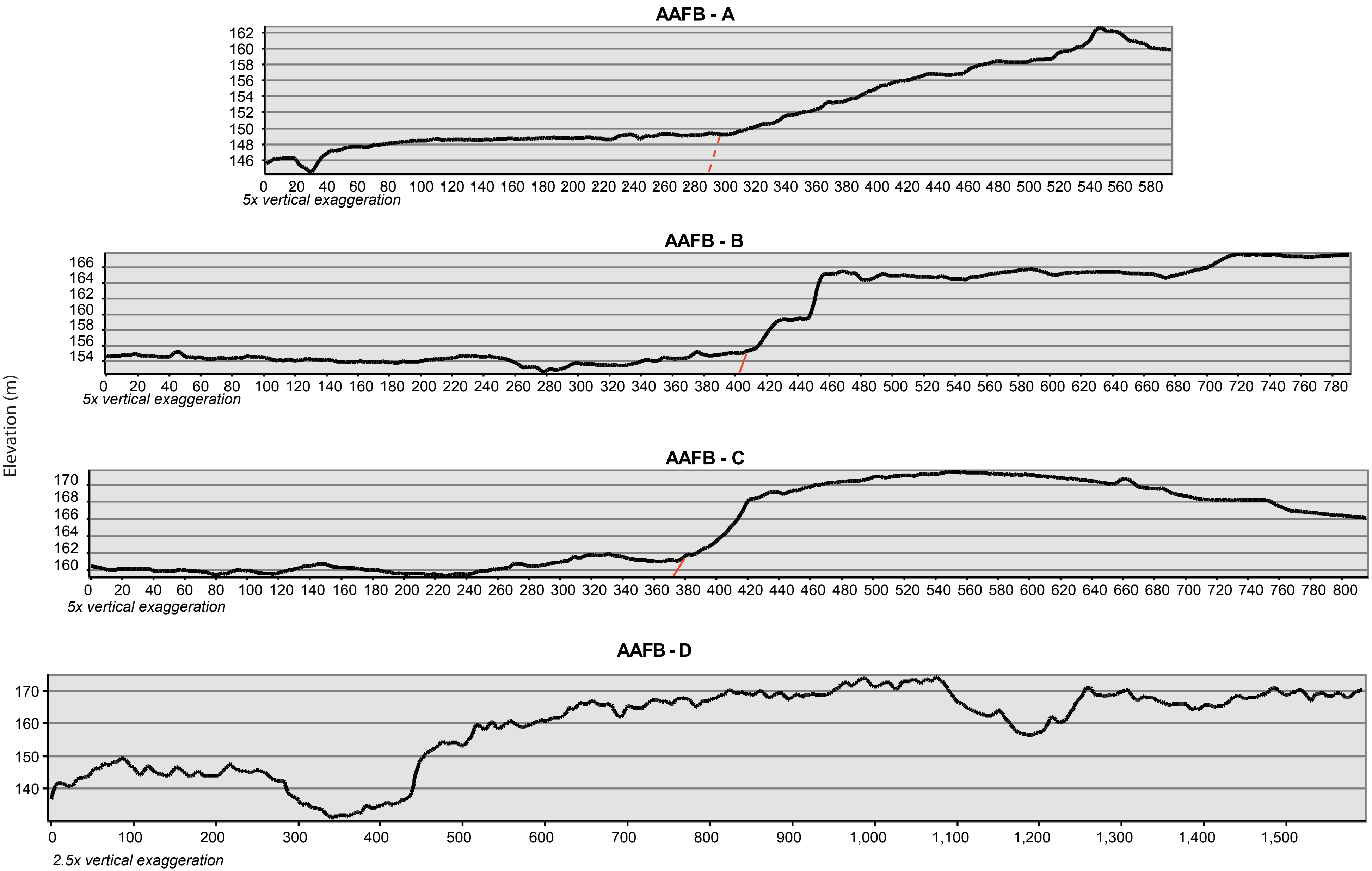

URS	Project No. 26818155 Fault Mapping in Guam	TOPOGRAPHIC PROFILES ACROSS AAFB FAULT, NORTHERN GUAM	Figure 9

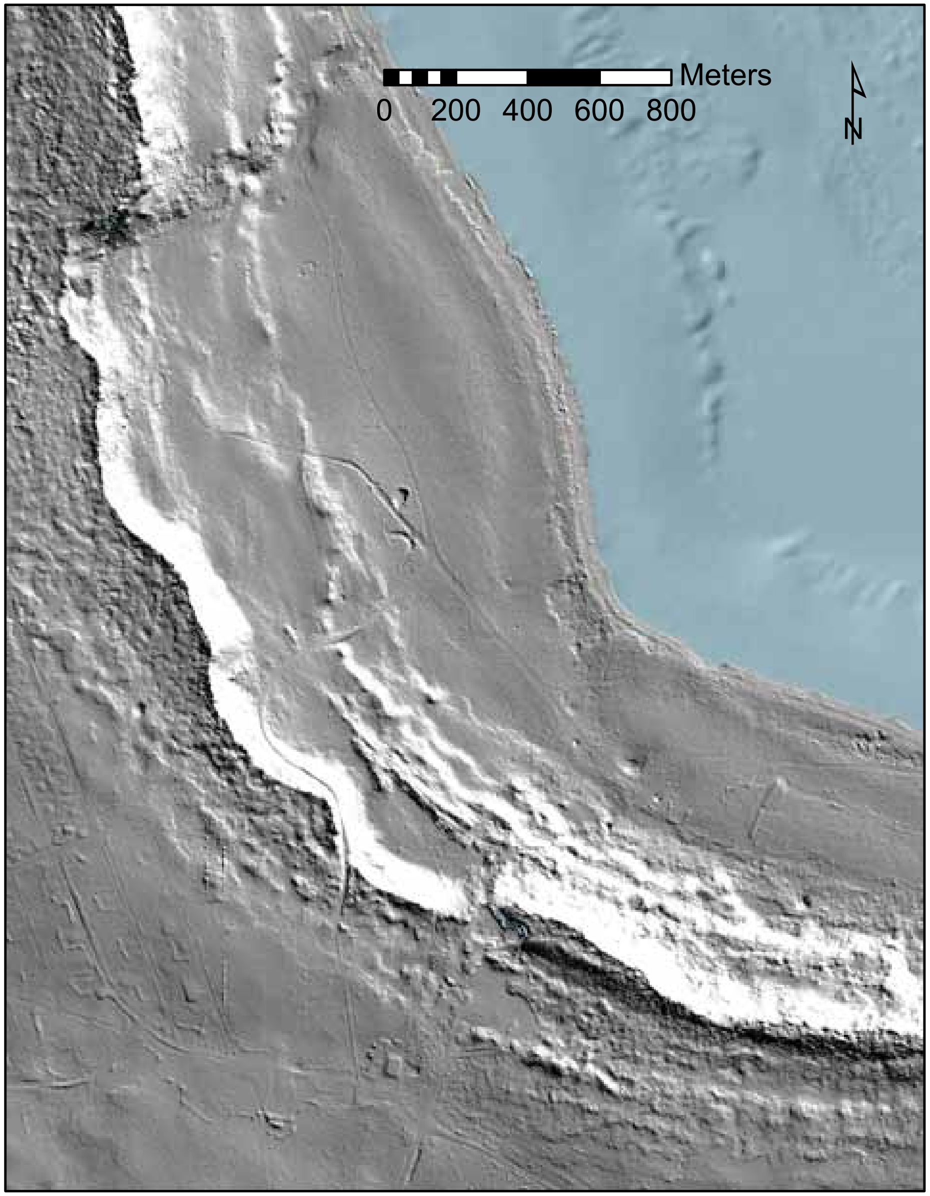

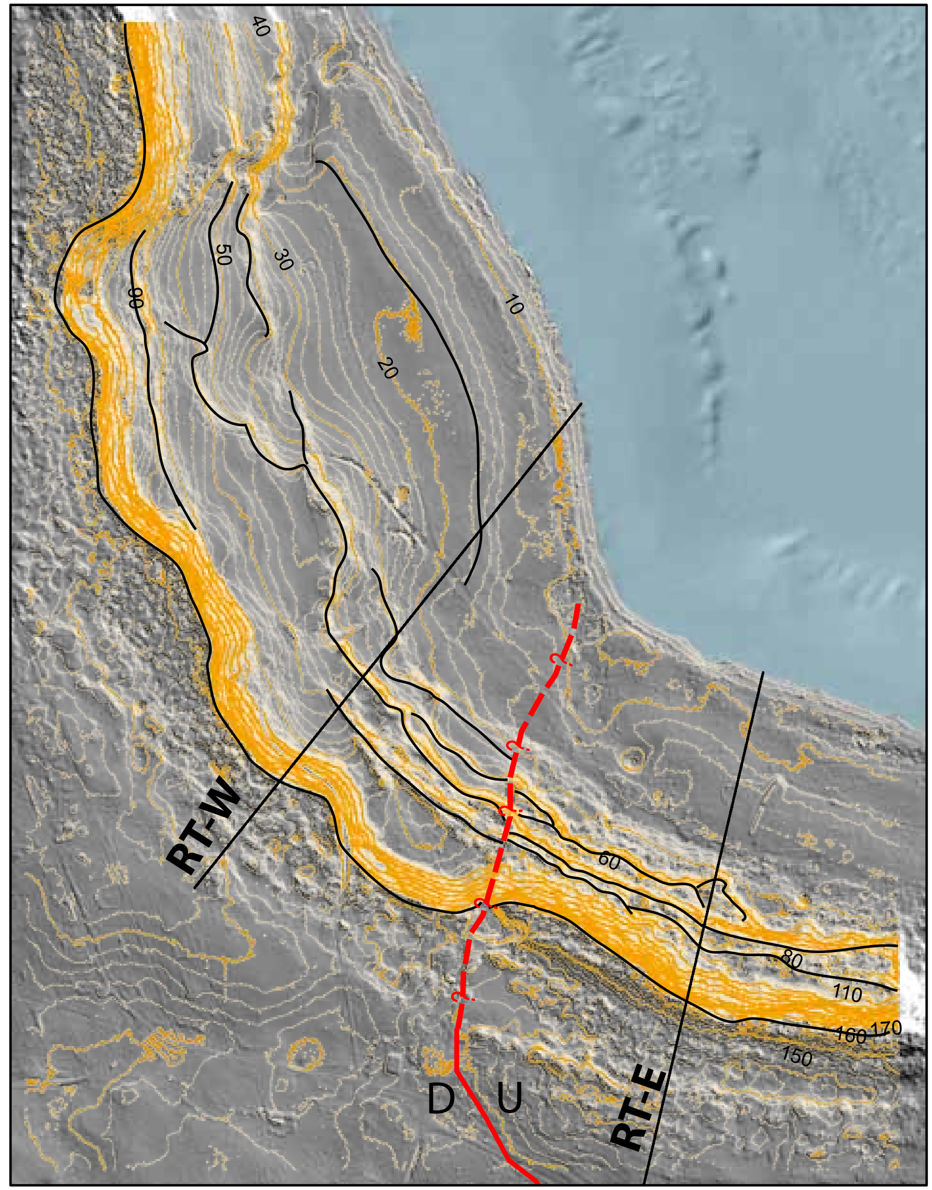

URS	Project No. 26818155 Fault Mapping in Guam	TOPOGRAPHIC PROFILES OF MARINE TERRACES ACROSS AAFB FAULT, NORTHERN GUAM	Figure 10

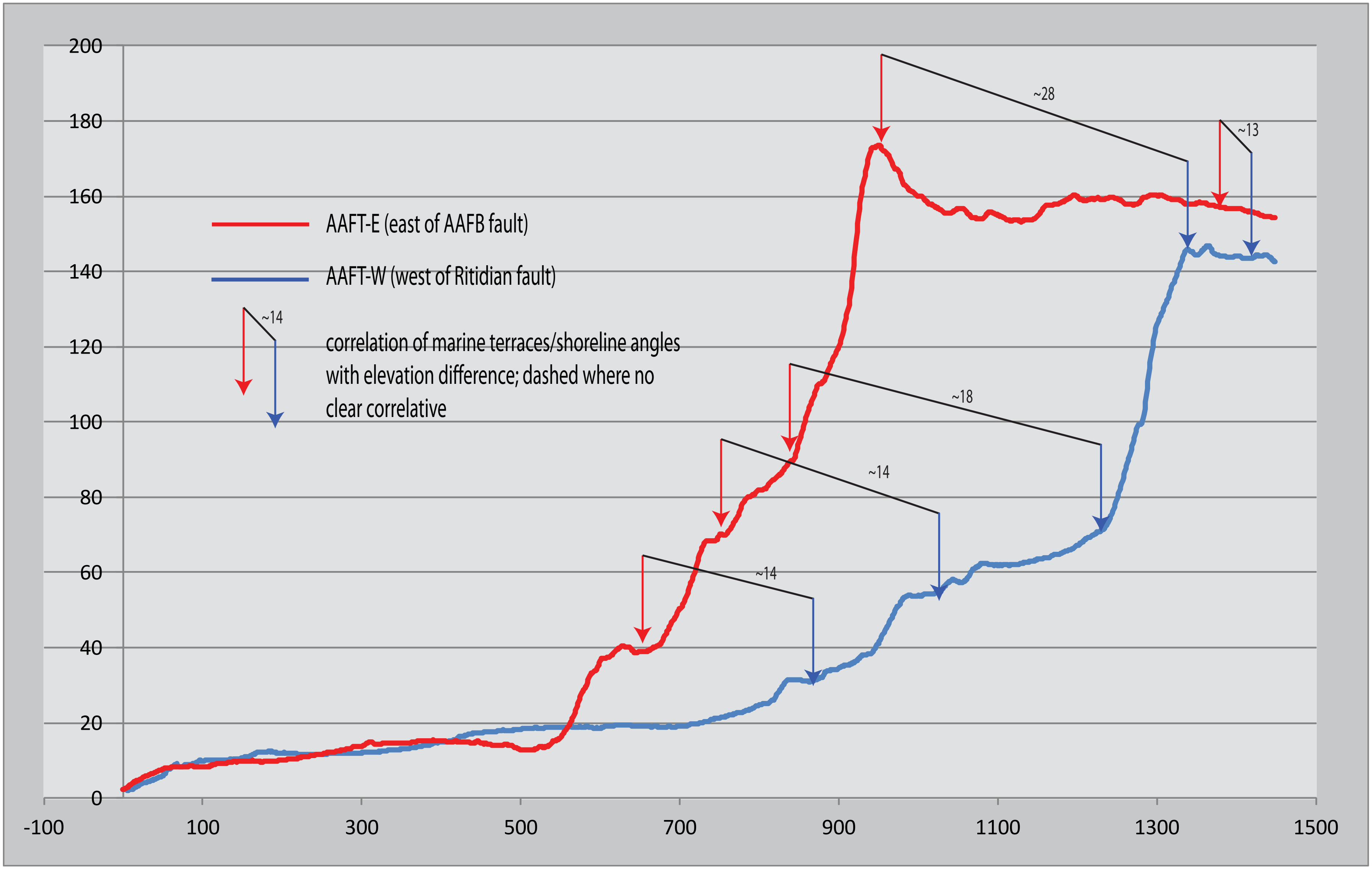

URS

Project No. 26818155

Fault Mapping in Guam

TOPOGRAPHIC PROFILES OF MARINE TERRACES ACROSS AAFB FAULT, NORTHERN GUAM

Figure 11

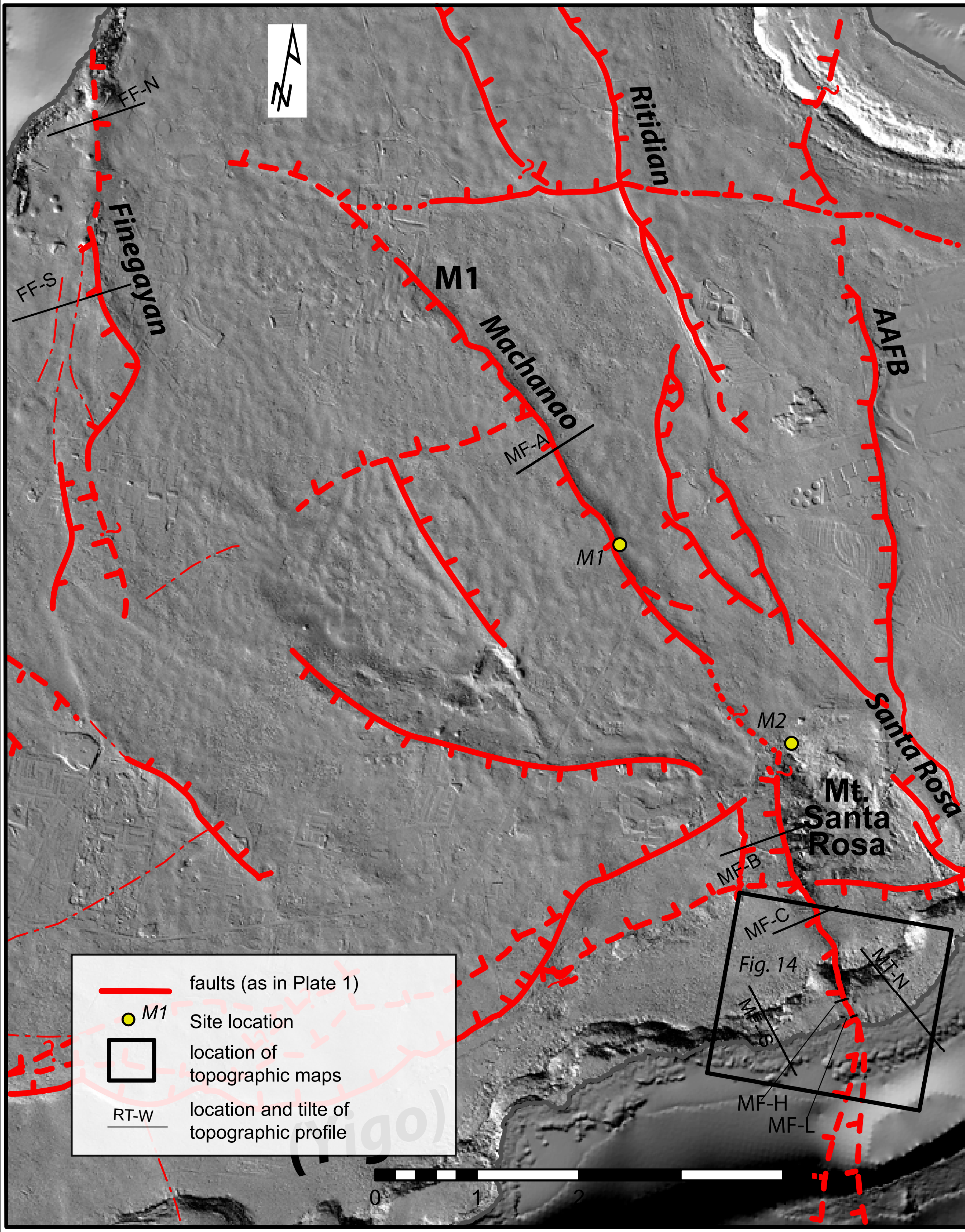

URS	Project No. 26818155	MAP OF MACHANAO AND FINEGAYAN FAULTS NORTHERN GUAM	Figure 12
	Fault Mapping in Guam		

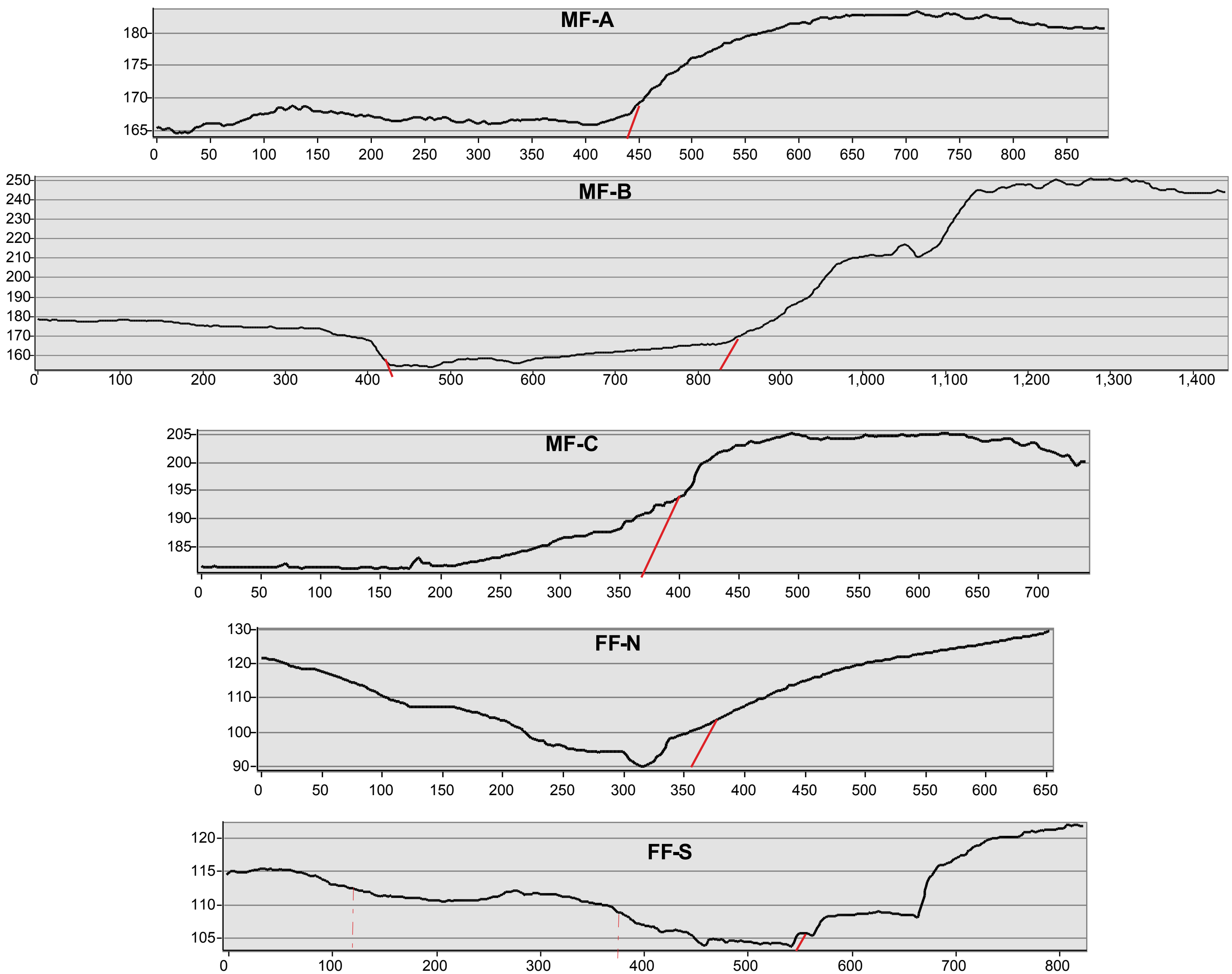

URS	Project No. 26818155 Fault Mapping in Guam	TOPOGRAPHIC PROFILES ACROSS MACHANAO AND FINEGAYAN FAULTS	Figure 13

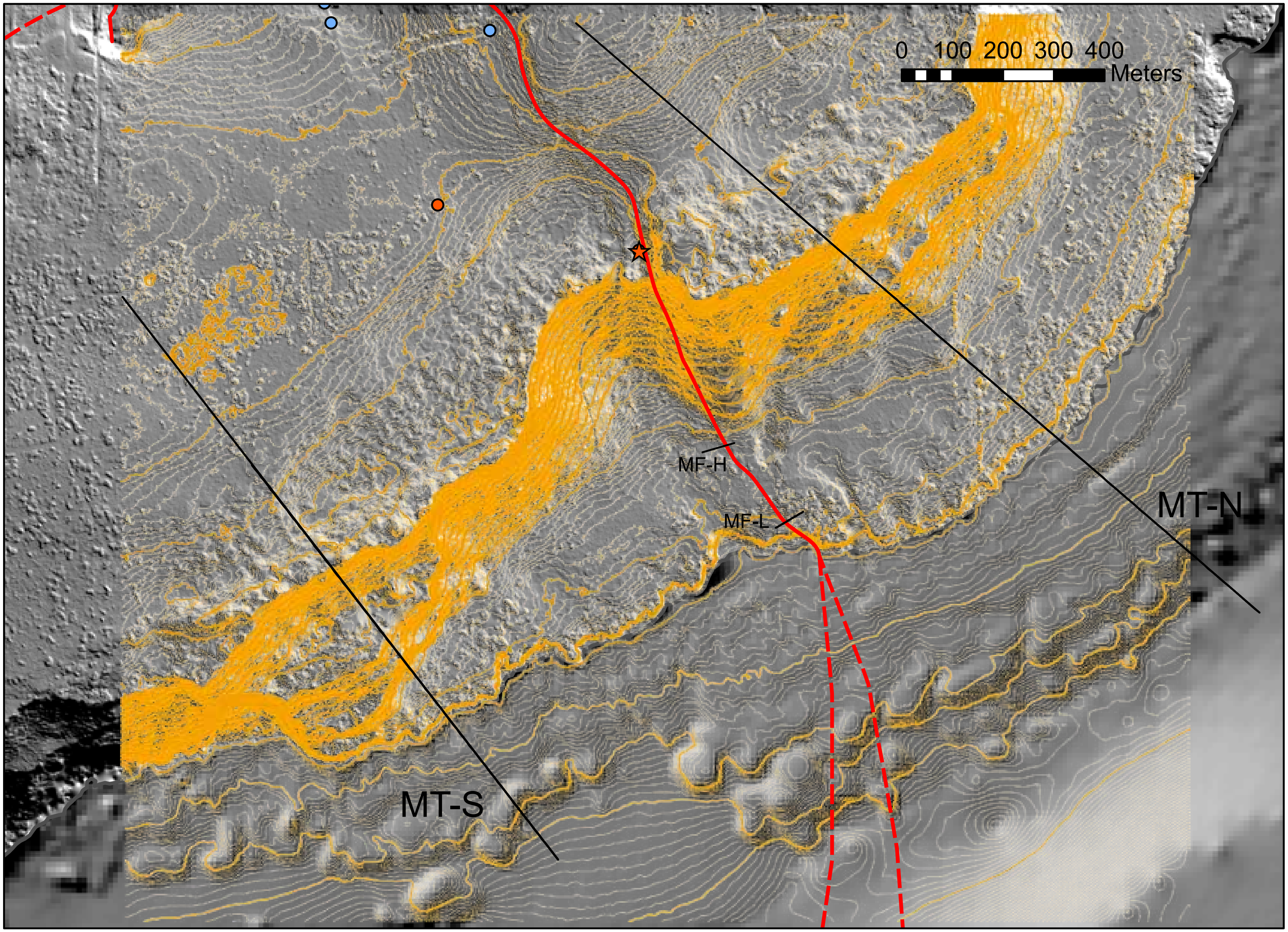

URS

Project No. 26818155

Fault Mapping in Guam

MARINE TERRACES DISPLACED BY THE MACHANAO FAULT, NORTHEAST GUAM

Figure 14

A. Scarp of Machanao fault at Site M1

B. Faulting in Alutom Fm. with unfaulted overlying alluvium at Site M2

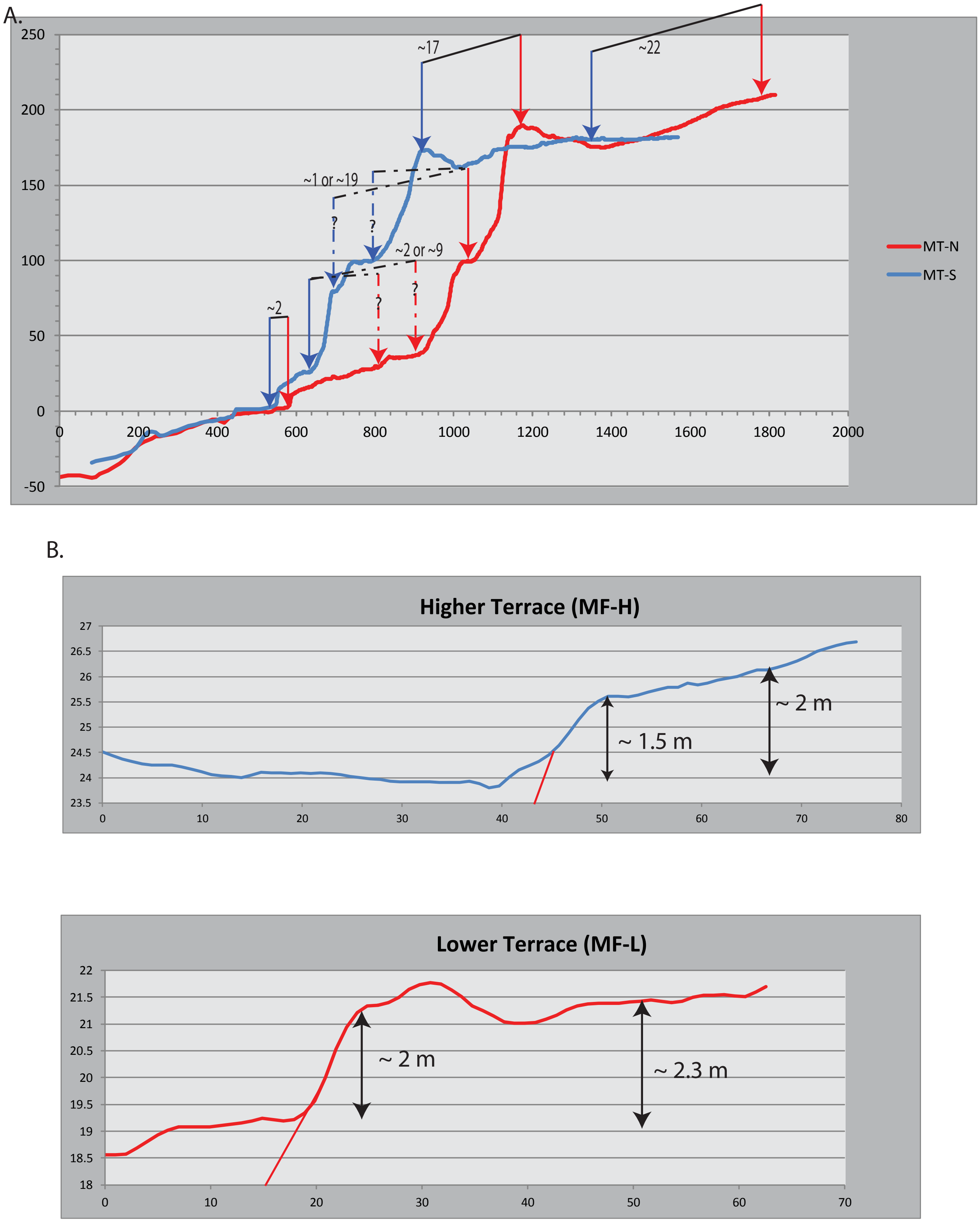

URS	Project No. 26818155 Fault Mapping in Guam	TOPOGRAPHIC PROFILES OF MARINE TERRACES AND ACROSS MACHANAO FAULT	Figure 16

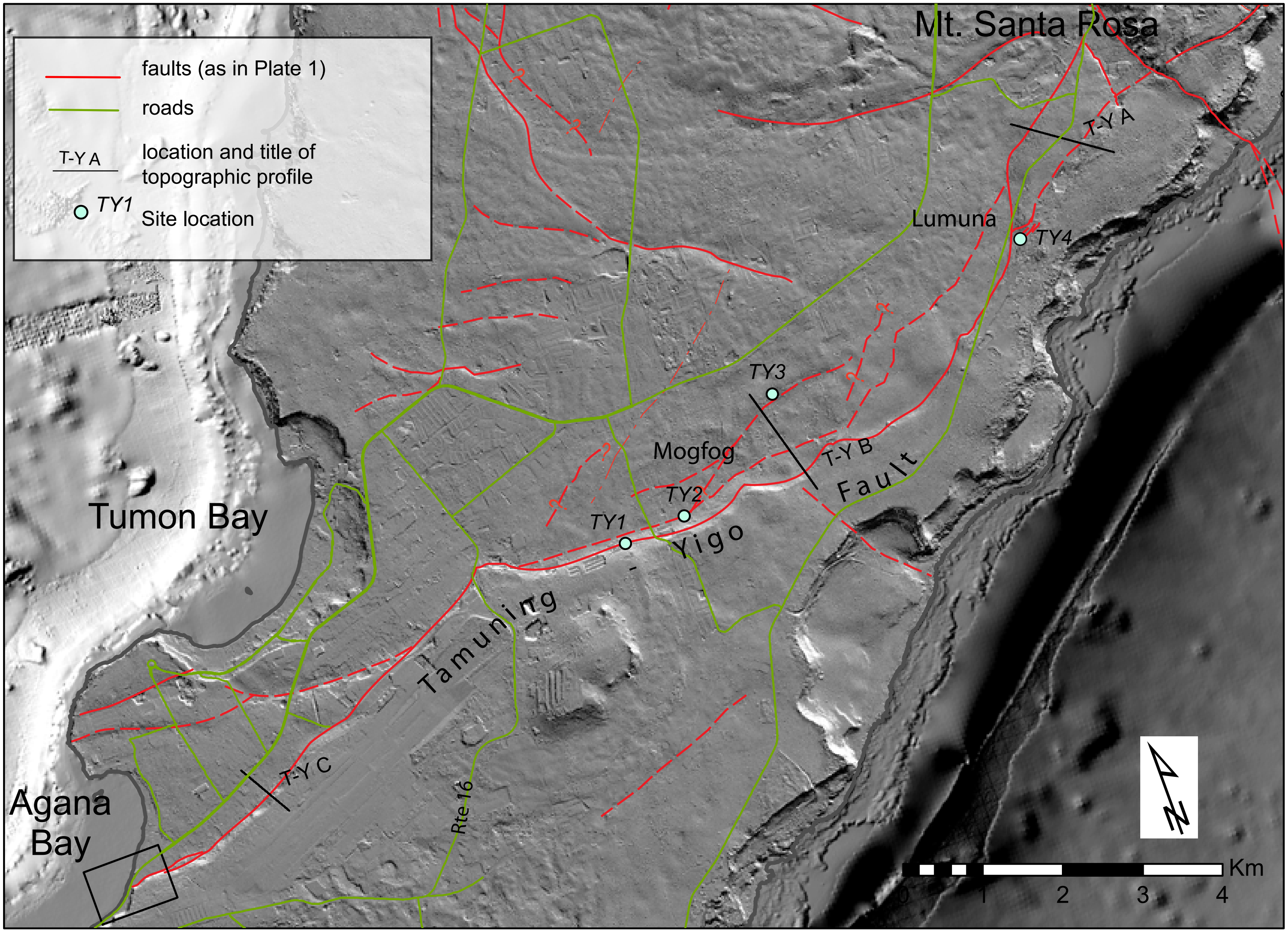

URS	Project No. 26818155 Fault Mapping in Guam	MAP OF TAMUNING-YIGO FAULT NORTHERN GUAM	Figure 17

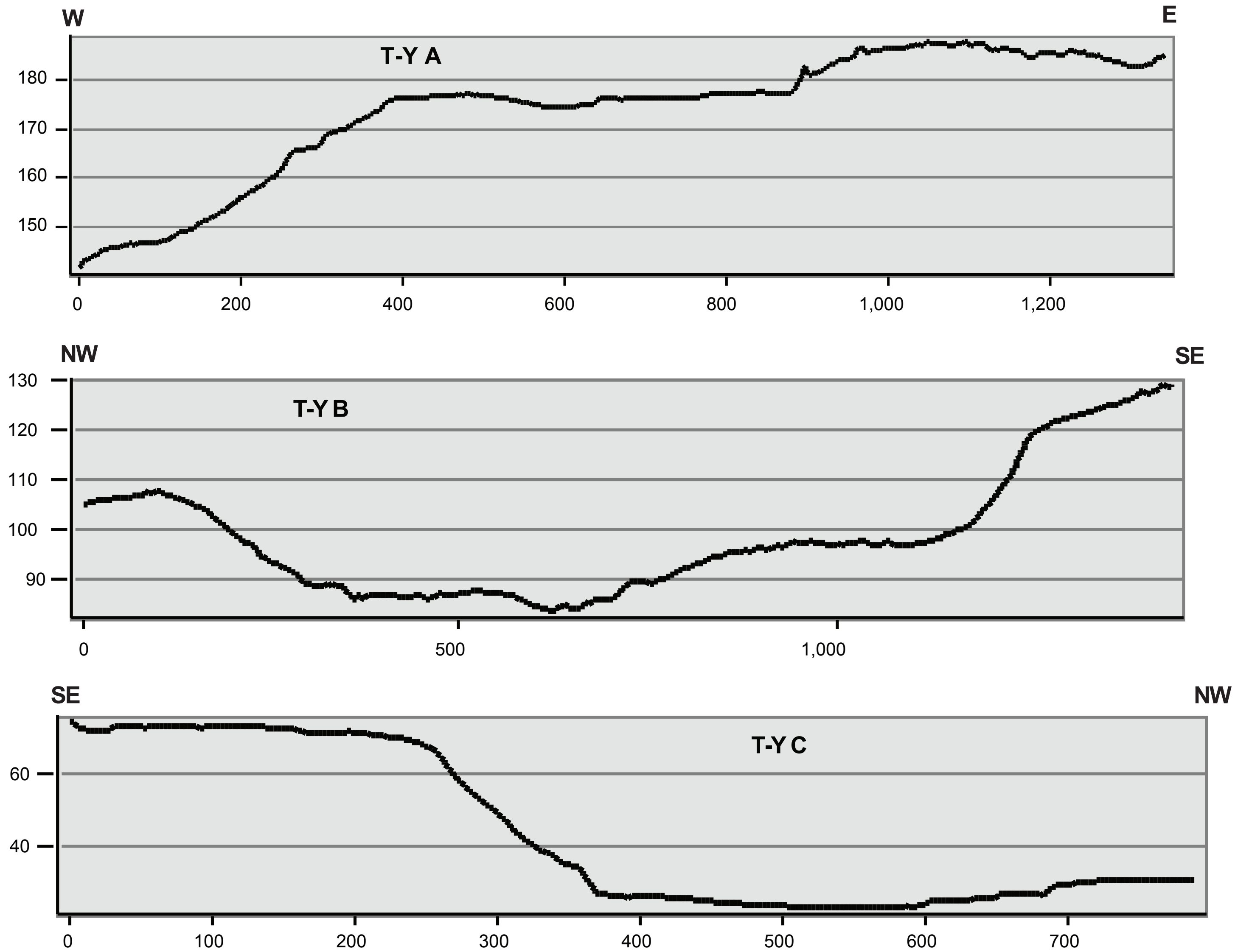

URS

Project No. 26818155

Fault Mapping in Guam

TOPOGRAPHIC PROFILES ACROSS TAMUNING-YIGO FAULT

Figure 18

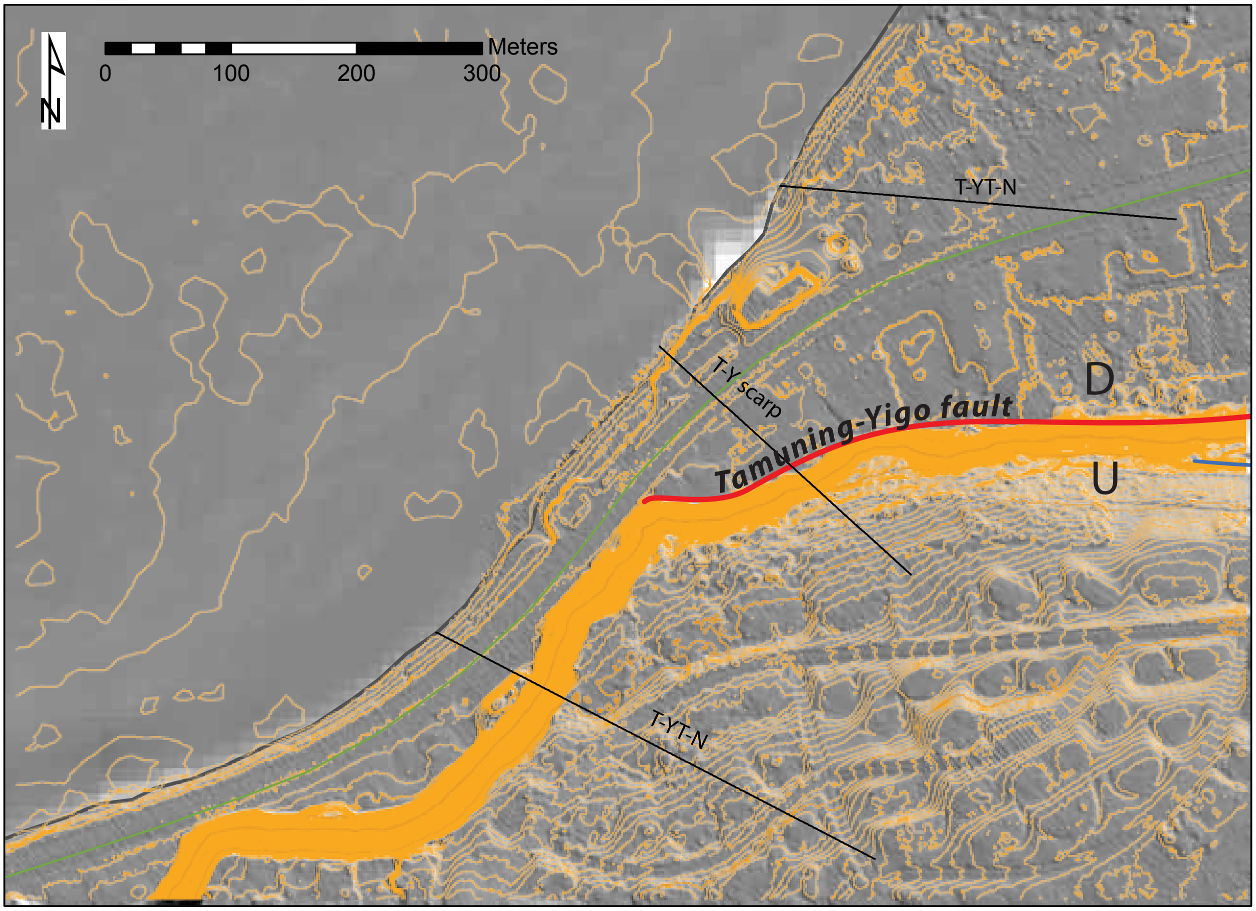

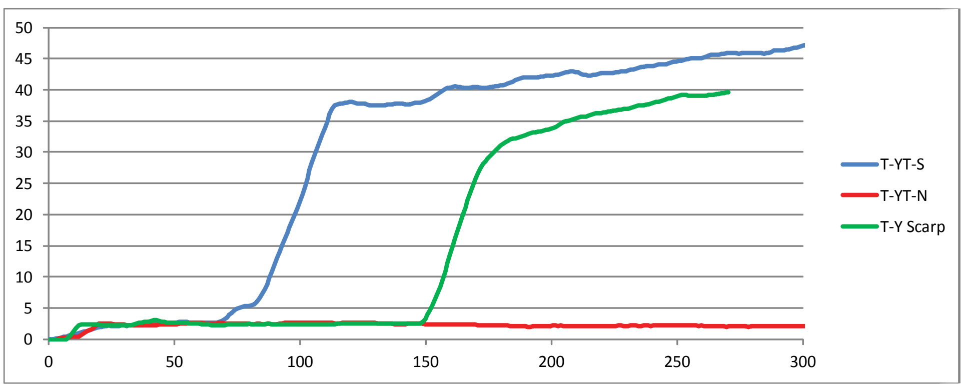

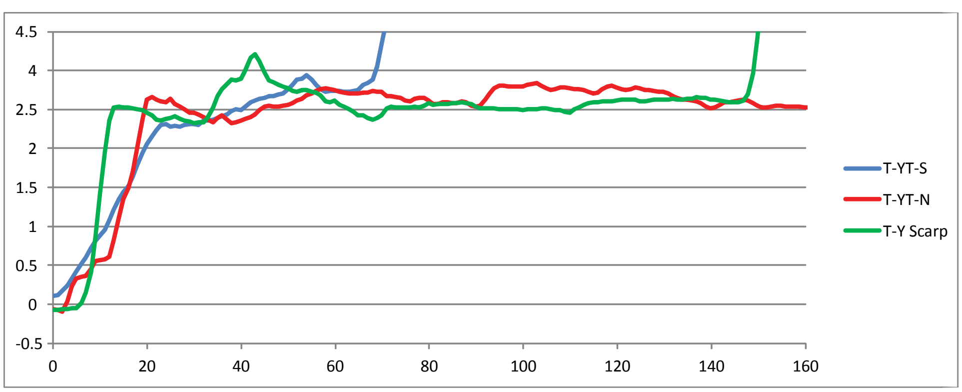

URS

Project No. 26818155

Fault Mapping in Guam

TOPOGRAPHIC MAP AND PROFILES OF MARINE TERRACES AND TAMUNING-YIGO FAULT AGANA BAY, GUAM

Figure 19

A.

Tamuning-Yigo fault in Mio-Pliocene Barrigada Limestone (TY1). Arrows point to bedrock fault and surface break in slope.

B.

Base of Tamuning-Yigo fault scarp near Mogfog (TY2)

C.

Tamuning-Yigo fault in limestone quarry near Lumuna (TY4)

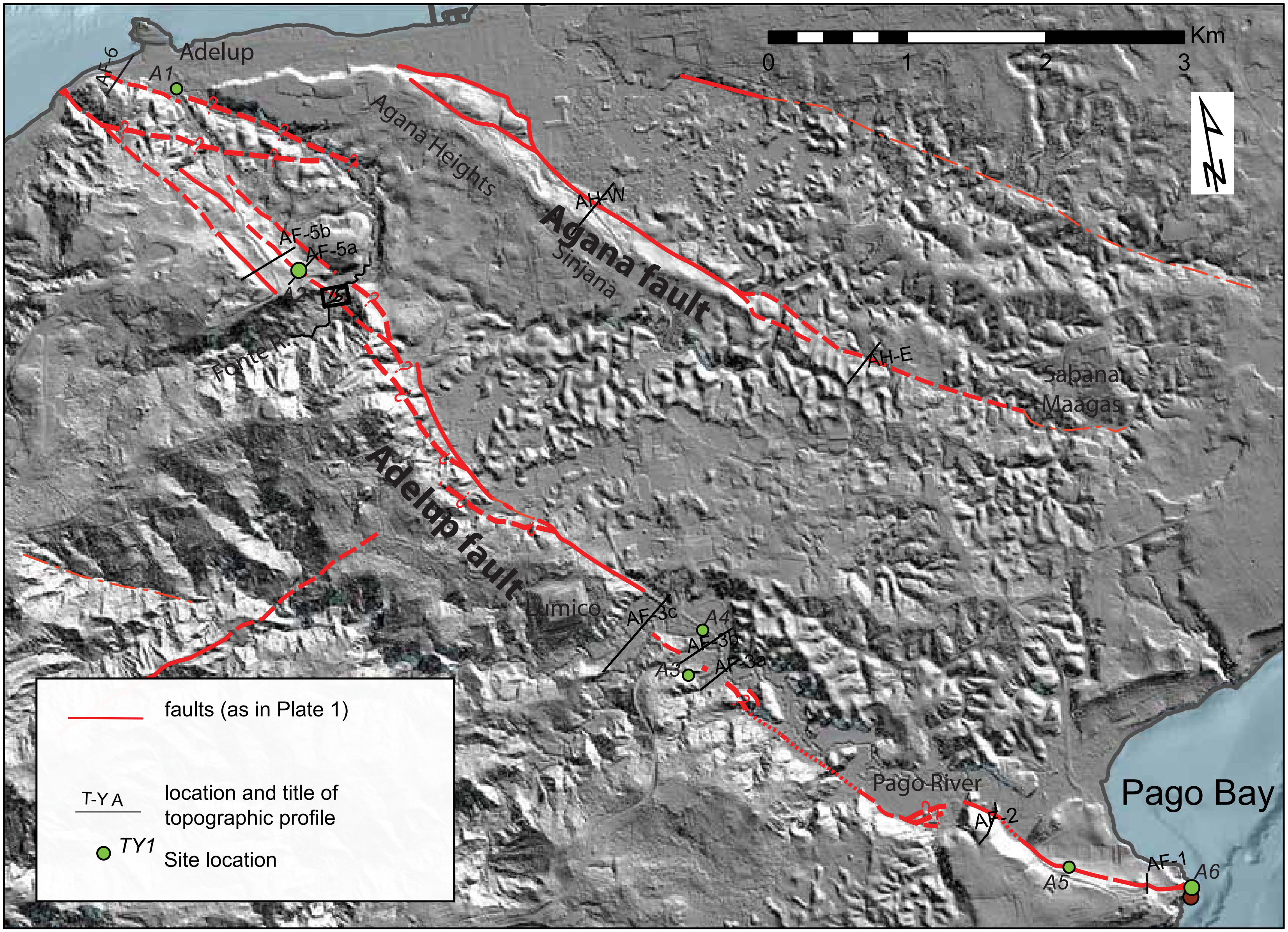

URS

Project No. 26818155

Fault Mapping in Guam

MAP OF ADELUP AND AGANA FAULTS

Figure 21

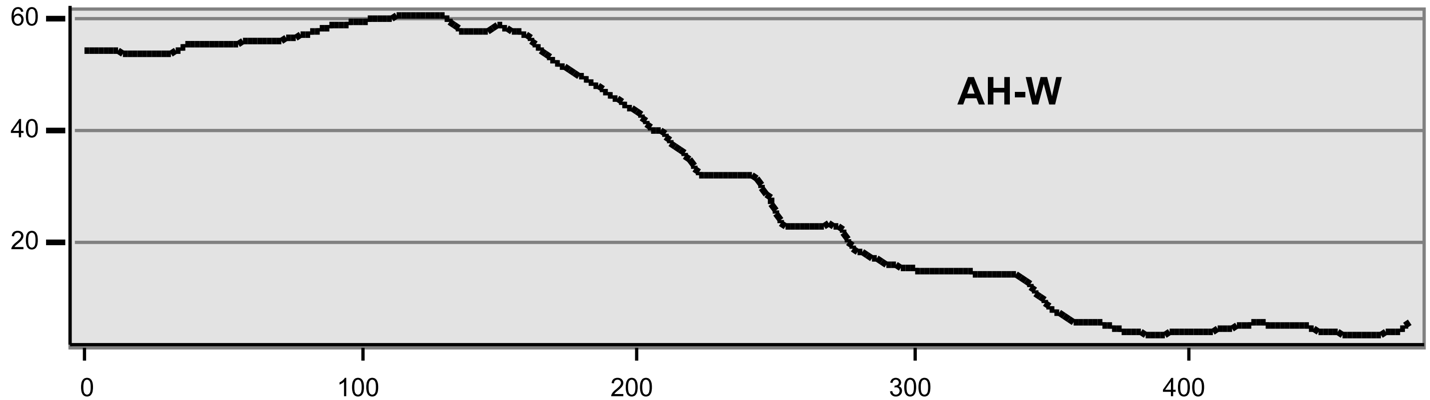

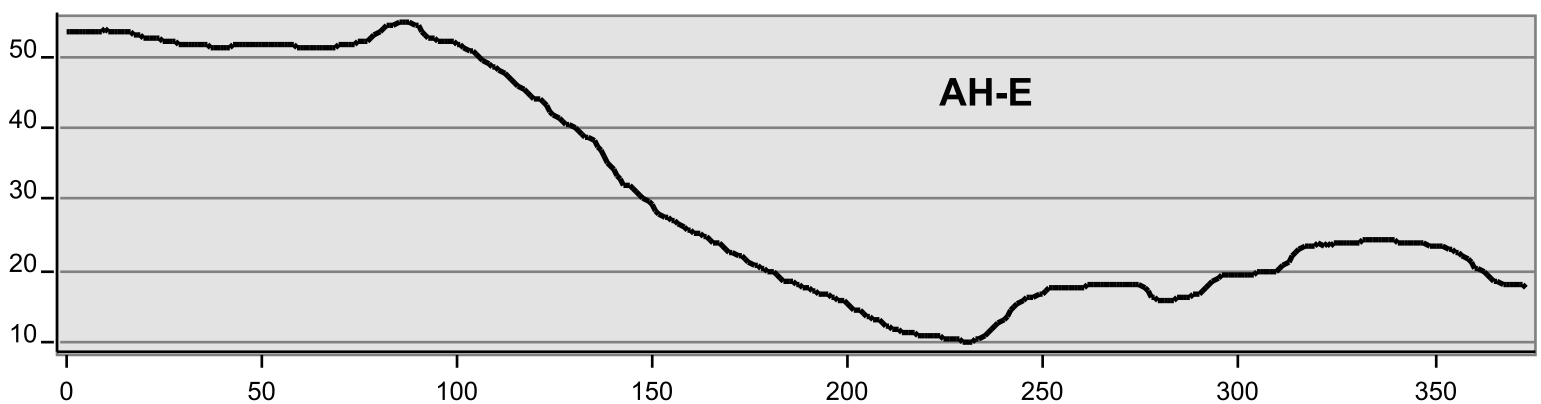

URS	Project No. 26818155 Fault Mapping in Guam	TOPOGRAPHIC PROFILE ACROSS AGANA FAULT	Figure 22

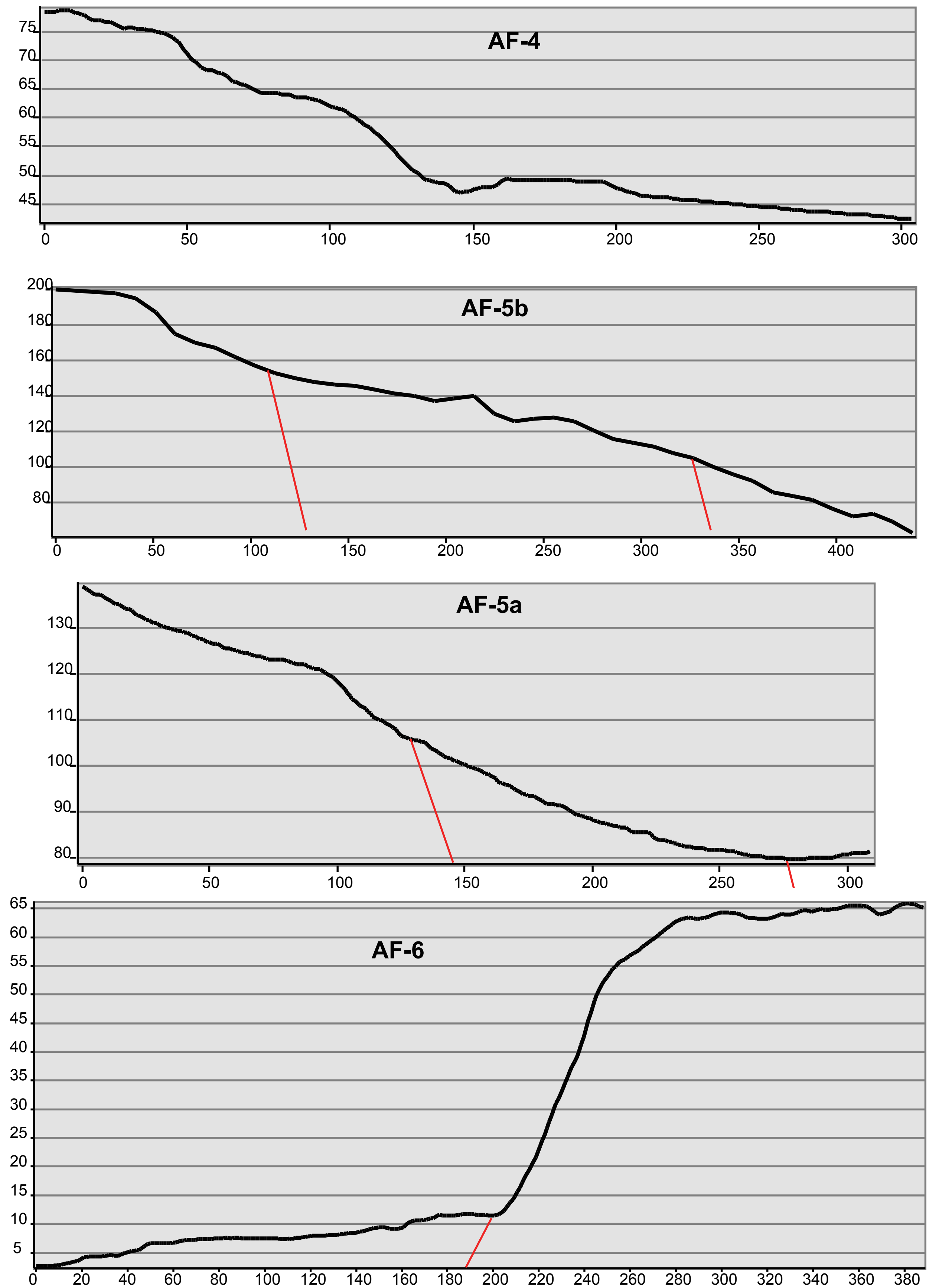

URS	Project No. 26818155	TOPOGRAPHIC PROFILES ACROSS ADELUP FAULT	Figure 22b
	Fault Mapping in Guam		

A

Steeply dipping mineralized shears in ALuton volcaniclastics.

B

1-2-m-high scarp on Holocene terrace deposits of the Pago RIver

A.

Adelup fault in Pago Bay Resort homeite (Lot 69)

B.

Bedrock fault extending across homesites into scarp. View to the west.

Double sea-level notch at Pago Point. Lower notch is modern; higher notch is Pleistocene (?).

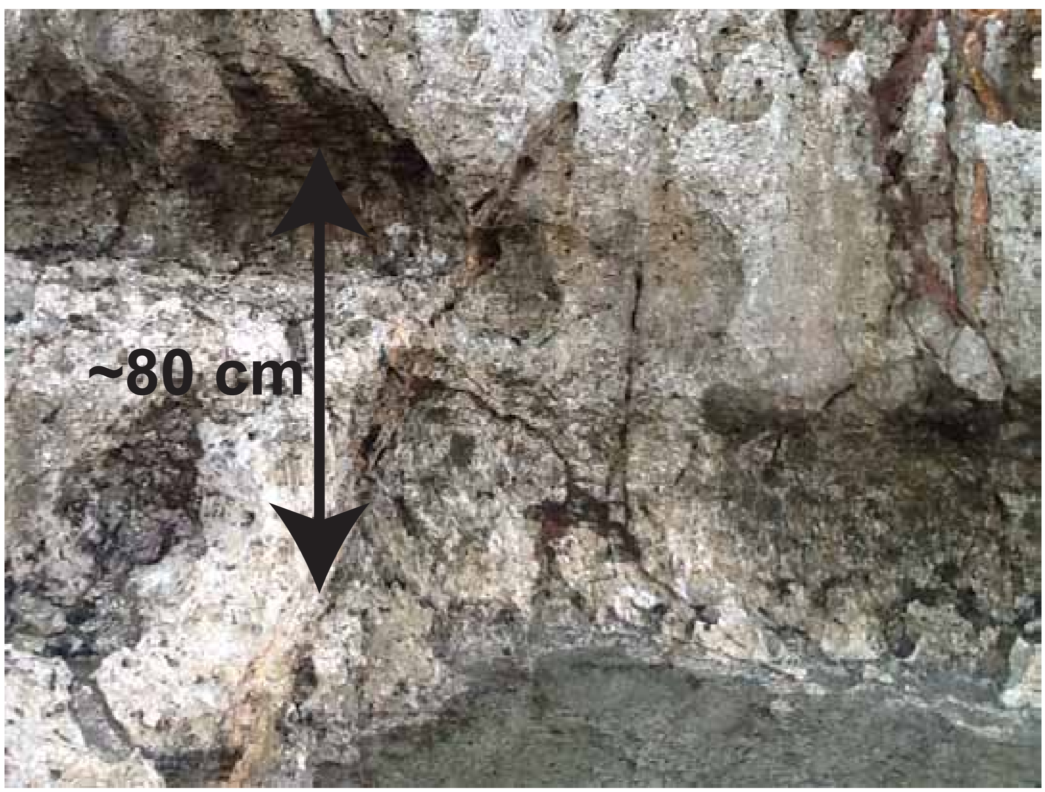

Adelup fault offsetting Holocene marine notch.

URS	Project No. 26818155	PHOTOGRAPHS ALONG ADELUP FAULT: OFFSET SEA-LEVEL NOTCHES AT PAGO POINT, CENTRAL GUAM	Figure 25
	Fault Mapping in Guam		